A Nematode-Selective Potentiator of Organophosphate and Carbamate Agrochemicals

Sean Harrington[1,2], Jessica J. Knox[2,3], Andrew R. Burns[2,3], Ken-Loon Choo[4], Aaron Au[2,5], Megan Kitner[6], Cecile Haeberli[7,8], Jacob Pyche[1,2], Cassandra D'Amata[2], Yong-Hyun Kim[4], Jonathan R. Volpatti[9,10], Maximillano Guiliani[2,5], Jamie Snider[2], Victoria Wong[2], Bruna M. Palmeira[11], Elizabeth M. Redman[11], Aditya S. Vaidya[12,13], John Gilleard[11], Igor Stagljar[2,3,14,15,16], Sean R. Cutler[12,13], Daniel Kulke[17, †,‡], James J. Dowling[9,10], Christopher M. Yip[2,5], Jennifer Keiser[7,8], Inga Zasada[6], Mark Lautens[4], and Peter J. Roy[1,2,3,20*]

[1]Department of Pharmacology and Toxicology, University of Toronto, Toronto, ON, M5S 1A8, Canada.

[2]The Donnelly Centre for Cellular and Biomolecular Research, University of Toronto, Toronto, ON, M5S 3E1, Canada.

[3]Department of Molecular Genetics, University of Toronto; Toronto, ON, M5S 1A8, Canada.

[4]The Department of Chemistry, University of Toronto, 80 St. George Street, M5S 3H6, Toronto, Canada.

[5]Institute of Biomaterials and Biomedical Engineering, University of Toronto, Toronto, Ontario, Canada.

[6]USDA-ARS Horticultural Crops Research Laboratory, Corvallis, OR 97330, USA.

[7]Department of Medical Parasitology and Infection Biology; Swiss-Tropical and Public Health Institute, (Swiss TPH), Socinstr. 57, CH–4051 Basel, Switzerland.

[8]Faculty of Science; University of Basel, Petersplatz 1, 4001 Basel.

[9]Program in Developmental and Stem Cell Biology, The Hospital for Sick Children, Toronto, Ontario, Canada M5G 0A4.

[10]Program in Genetics and Genome Biology, The Hospital for Sick Children, Toronto, Ontario, Canada M5G 0A4.

[11]Department of Comparative Biology and Experimental Medicine, Host-Parasite Interactions (HPI) Program, Faculty of Veterinary Medicine, University of Calgary, Calgary, AB, Canada.

[12]Institute for Integrative Genome Biology, University of California, Riverside, Riverside, CA 92521, USA.

[13]Department of Botany and Plant Sciences, University of California, Riverside, Riverside, CA 92521, USA.

[14]Department of Biochemistry, University of Toronto, Toronto, ON, M5S 1A8, Canada.

[15]Mediterranean Institute for Life Sciences, Meštrovićevo Šetalište 45, HR-21000, Split, Croatia.

[16]School of Medicine, University of Split, Šoltanska ul. 2, 21000, Split, Croatia.

[17]Research Parasiticides, Bayer Animal Health GmbH, Monheim, Germany.

[†]Current affiliation, Department of Biomedical Sciences; Iowa State University, Ames, Iowa 50011, USA.

[‡]Current affiliation, Global Innovation, Boehringer Ingelheim Vetmedica GmbH; Binger Str. 173, 55218 Ingelheim am Rhein, Germany.

*Corresponding author. Email: peter.roy@utoronto.ca

One-Sentence Summary: A *C. elegans*-based screening pipeline identifies a selective nematicide that potentiates acetylcholinesterase inhibitors.

ABSTRACT

Nematode parasites of humans, livestock and crops pose a significant burden on human health and welfare. Alarmingly, parasitic nematodes of animals have rapidly evolved resistance to anthelmintic drugs, and traditional nematicides that protect crops are facing increasing restrictions because of poor phylogenetic selectivity. Here, we present a pipeline that exploits multiple motor outputs of the model nematode *C. elegans* for nematicide discovery. This pipeline yielded a compound, which we call Nementin, that selectively immobilizes diverse nematode parasites. We find that Nementin induces convulsions by agonizing neuronal dense core vesicle release, which in turn agonizes cholinergic signaling. Consequently, Nementin synergistically enhances the potency of acetylcholinesterase inhibitors that are restricted agrochemicals. Nementin therefore represents a novel candidate nematicide that may improve the selectivity of broad-acting pesticides.

INTRODUCTION

Parasitic nematodes are a scourge to humanity. Not only do helminths currently infect more than 1.5 billion people (WHO Soil Transmitted Helminth Fact Sheet, 2022) but nematode parasitism also destroys tens of billions of dollars (USD) worth of livestock annually (*1*). Alarmingly, the rate of destruction is growing due to the evolution of anthelmintic resistance (*2*). Plant-parasitic nematodes (PPNs) are even more destructive as they ruin over 125 billions of dollars (USD) worth of food crops annually (*3*). Traditional nematicides that protect crops have been justifiably banned or severely restricted due to a lack of phylum selectivity(*4*), but these restrictions severely impact food security (*5*). Compounding these issues, global food demand is expected to increase by 70% by the year 2050 (*6*). Hence, the development of new and selective nematicides is essential to our collective welfare.

Here, we present a novel motor-centric screening pipeline to identify novel candidate nematicides. Disrupting a parasite's motor control has repeatedly proven effective in mitigating nematode infection (*7, 8*). We therefore screened our collection of worm-active (wactive) compounds (*9*) using two successive behavioural assays of the free-living nematode *Caenorhabditis elegans*. We identified four molecules that fail to elicit phenotypes in off-target systems at concentrations that kill multiple nematode species. We focused on one of these, called Nementin, that induces *C. elegans* hyperactivity within seconds of exposure, followed by whole-body convulsions minutes later. Nementin and its analogs selectively immobilize and/or kill nematode parasites of plants and mammals. Chemical-genetic analyses reveal that Nementin agonizes neuronal

dense core vesicle release, which in turn, agonizes synaptic vesicle release. This insight led to the finding that Nementin enhances the paralytic effects of organophosphate and carbamate acetylcholinesterase inhibitors not only in *C. elegans*, but in nematode parasites of mammals and plants. We conclude that Nementin is a novel nematode-selective scaffold that may also improve the selectivity of broad-acting pesticides.

RESULTS

26 Compounds Disrupt Multiple *C. elegans* Motor Activities

To identify small molecules that disrupt nematode neuromuscular activity, we designed a 96-well plate imaging system that measures the egg-laying rate of adult *C. elegans* hermaphrodites (Fig. S1). The regulation of *C. elegans* egg-laying relies on well-characterized cholinergic, serotonergic, GABAergic and peptidergic circuits (*10*), and is therefore a paragon to assess neuromuscular perturbation by small molecules. Using methodology described in the Supplementary Text, we screened our collection of 486 worm-active (wactive) compounds (*9*) and identified 29 stimulators and 29 inhibitors of egg-laying (Fig. 1A; Data S1; Data S2). A Tanimoto structural similarity cut-off of 0.55 reveals that the 58 egg-laying modulators segregate into 11 clusters and 26 singletons that have a distinct structural scaffold (Fig. 1A). 10 of the 11 clusters are composed of molecules with the identical egg-laying phenotype, which validates the phenotypic assignments.

We reasoned that molecules that disrupt multiple motor circuits are more likely to break the parasitic nematode lifecycle. We therefore surveyed the 58 egg-laying modulators for those that disrupt the normal sinusoidal locomotion of wild type *C. elegans*. 26 of the 58 egg-laying modulators (45%) induce at least one locomotory phenotype such as convulsions, coiling, and paralysis (Table 1; Fig. 1A; Movies S1-S6; Data S3). The molecules that induce slow movement and paralysis are dominated (88%) by molecules that inhibit egg-laying (Fig. 1A; Table 1). This is consistent with the idea that the egg-laying inhibitor class may be enriched with acutely lethal molecules

(Fig S1). By contrast, the molecules that induce convulsions, shaking, and coiling are dominated (80%) by those that enhance egg-laying (Table 1).

Nementin-1 is Effective Against Multiple Parasitic Nematodes

To prioritize the 26 neuromodulatory molecules, we eliminated those from consideration that: i) are cytotoxic to human HEK293 cells; ii) induce developmental defects in zebrafish; iii) have lackluster lethality against the five nematodes previously assayed; iv) induce subtle locomotory phenotypes (reversal-defective), or v) were closely related to the commercial nematicide fluopyram (*9*) (Table 1; Data S4). This left worm-active (wact) molecules 10, 13, 15, 55, 120, 128, and 444 for further consideration (Fig. 1B; Table 1).

We further assessed the activity of our seven hits against seven nematode species from three phylogenetic clades (Fig. 1C). Four of these seven species are parasitic. We also analyzed (or reanalyzed) the molecules' activity against the non-target models *D. rerio* fish, HEK293 cells, and *Arabidopsis thaliana* plants (Fig. 1C; Fig. S2). We prioritized wact-55 because it arguably demonstrates the best combination of broad nematode activity and selectivity. SciFinder-based literature searches failed to reveal prior annotation of nematicidal activity for wact-55's alkyl phenylpiperidine core scaffold (*11*).

A detailed temporal analysis showed that within 90 seconds of exposure of 60 μM wact-55, *C. elegans* exhibits a hyperactive nose movement phenotype (Fig. 1D). The hyperactive phenotype dissipates at the expense of spastic convulsions over the course

of 2 hours (Fig. 1D). By 24 hours, 100% of the adult animals incubated in wact-55 are dead (non-moving and/or disintegrating; three trials, n = 18 animals per trial). We renamed the wact-55 molecule 'Nementin-1' (nematode enhancer of neurotransmission-1).

To determine whether Nementin-1 might have a canonical mechanism-of-action (MOA), we tested whether any of the *C. elegans* mutant strains that resist the effects of seven popular anthelmintics also resist the lethal effects of Nementin-1. All drug-resistant strains remain sensitive to Nementin-1 (Fig. S3). Furthermore, we previously showed that *C. elegans* cannot be easily mutated to resist Nementin-1's lethality; 290,000 randomly mutated genomes failed to yield wact-55-resistant mutants (*9*). These results suggest that: i) Nementin-1 does not share an MOA with canonical anthelmintics, ii) Nementin-1's MOA may not be limited to a single protein target, and, iii) genetic resistance to Nementin-1 may be difficult to achieve in the field. All of these properties make Nementin-1 an attractive hit for further investigation.

Nementin Convulsions are Dependent on Dense Core Vesicle Release

We reasoned that mutations in the pathway targeted by Nementin-1 might phenocopy the motor defects induced by the molecule and provide mechanistic insight. A survey of the literature yielded eight mutants that share at least some of Nementin-1's phenotypes, including *acr-2, unc-2, unc-43, unc-58, unc-93, sup-9, sup-10*, and *twk-18* (*12-20*) (Table S1). We tested the hypothesis that Nementin-1 disrupts the pathway disrupted by each of these mutants. We did this by asking whether known suppressors

of the phenocopying mutants can suppress Nementin-1's effects (see Table S1). Of the potential suppressing mutants tested, only the *unc-43* gain-of-function (GF) mutant resisted Nementin-1's convulsions (Fig. 2A). We also found the converse to be true; *unc-43* reduction-of-function (RF) alleles enhance Nementin-1 convulsions (Fig. 2A). Remarkably, the interaction between the *unc-43* GF and Nementin-1 is mutual in that Nementin-1 can rescue the paralysis of *unc-43* GF (Fig. 2B). This observation argues against the idea that the *unc-43* GF mutant alters Nementin-1 absorption or metabolism. These results suggest that Nementin-1 may be disrupting UNC-43 pathway activity.

UNC-43 is the *C. elegans* ortholog of CaMKII (calcium/calmodulin-dependent protein kinase II) and is a key negative regulator of dense core vesicle (DCV) release in *C. elegans* neurons (*13, 21*) (Fig. 2C). In animals with reduced UNC-43 function, neuronal DCV content is released in excess and is likely responsible for the mutant's convulsive and constitutive egg-laying phenotypes (*12, 21*). In *unc-43* GF animals, DCVs accumulate, and their limited release is likely responsible for the mutant's severely lethargic locomotion (*21*).

To examine DCV behaviour in response to Nementin-1, we exploited the neuropeptide reporter (INS-22::GFP) that is packaged into DCVs in cholinergic motor neurons (*21*). Like *unc-43* RF mutants (*21*), worms treated with either Nementin-1 or a second analog called Nementin-12 have reduced axonal INS-22::GFP signal ($p<0.05$) (Fig. 2D-2H; Fig. S4). Coincidentally, INS-22::GFP accumulates in the pseudocoelomic fluid-scavenging cells, called coelomocytes, of Nementin-treated animals (Fig. 2H; Fig. S4).

We reasoned that if Nementin disrupts motor behavior by agonizing DCV release, then disruption of UNC-31 (calcium-dependent activator protein for secretion (CAPS)), which is required for DCV release (*21, 22*), or UNC-64 syntaxin, which is required for all vesical fusions (*23, 24*), should suppress the Nementin-1-driven locomotory defects. Indeed, we find that both the weaker temperature-sensitive *unc-31(e169)*, the *unc-31(e928)* null, and the canonical *unc-64(e246)* RF mutants suppress the convulsions induced by Nementin-1 (Fig. 2A). Together, these data indicate that Nementin-induced DCV release is responsible for convulsions.

Collectively, these results beg the question of whether UNC-43 is likely to be the physiologically relevant target of Nementin-1. Several observations argue against this. First, we note that the terminal phenotype of Nementin-1 is death, yet presumptive null alleles of *unc-43* (*ce685* and *n1186*) are viable (*13, 21*). Second, if Nementin-1 inhibits UNC-43, then Nementin-1 should not be able to enhance the convulsion phenotype of *unc-43* null mutants. We find that Nementin-1 does indeed enhance presumptive *unc-43* null mutants (*ce685* and *n1186*) (Fig. 2A). Third, if UNC-43 was Nementin-1's sole physiological target, then *unc-43* GF mutations would have been identified in our genetic suppressor screens (*9*), but no resistant mutants arose. Finally, the *unc-43* GF mutant (and *unc-31* and *unc-64* RF mutants) remain sensitive to the lethal effects of Nementin-1 (Fig. S5). Together, these data argue against the idea that UNC-43 is Nementin-1's sole physiologically relevant target. Instead, the similarities between Nementin-1-induced phenotypes and the *unc-43* RF mutants suggest that the compound targets a component(s) that acts with UNC-43 (Fig. 2C, purple glow).

Nementin-1 Agonizes Cholinergic Signaling

We next investigated whether cholinergic signaling is also required for Nementin-1 activity. We tested whether mutants of the UNC-17 vesicular acetylcholine transporter (VAChT), which loads synaptic vesicles (SVs) with acetylcholine, or mutants of UNC-13, which is specifically required for SV release (*25, 26*), could suppress Nementin-1-induced convulsions. Reduction-of-function mutants of UNC-17 and UNC-13 remained sensitive to Nementin-1 (Fig. 3A). Incidentally, we found that Nementin-1 could partially rescue the lethargic locomotion of *unc-17* RF mutants (Fig. 3B). These data show that despite cholinergic signalling being dispensable for Nementin-1-induced convulsions, Nementin-1 may nevertheless agonize cholinergic signalling.

We further investigated the idea that Nementin-1 agonizes cholinergic signalling. To do so, we used the acetylcholinesterase (AChE) inhibitor aldicarb, which is a well-characterized tool used to investigate perturbations of cholinergic signaling in *C. elegans* (*27*). AChE catabolizes acetylcholine at the neuromuscular junction (NMJ) and its inhibition increases acetylcholine levels that in turn paralyzes the animal (*28*) (see Fig. 2C). We found that Nementin-1 sensitizes animals to the paralytic effects of aldicarb (Fig. 3C), suggesting that Nementin-1 agonizes acetylcholine release at the NMJ. The relationship between Nementin-1 and aldicarb is synergistic in nature, yielding a zero-interaction potency (ZIP) δ-score of 31.1 with a δ-score of 64.8 over the most synergistic set of concentrations (ZIP scores >10 are considered synergistic (*29, 30*) (Fig. 3D). Nementin-1 also enhances the paralysis induced by dichlorvos and trichlorfon, which are two other AChE inhibitors that are also commercial anthelmintics, by 12.7 and 18.7-fold, respectively (Fig. 3C). By contrast, Nementin-1 fails to enhance

the effects of an AChE-inhibitor on the fruit fly *D. melanogaster* (Fig. 3C). These data provide additional support for the idea that Nementin-1 agonizes cholinergic signalling and does so in a nematode-selective manner.

Cholinergic Agonism is a Secondary Effect of DCV Release

Neuropeptides released from DCVs are known to interact with G-protein coupled-receptors (GPCRs) that signal through G-proteins (*31*). In *C. elegans* neurons, the $G\alpha_q$ protein EGL-30 stimulates DAG production via the EGL-8 and PLC-3 phospholipases (*32*) (see Fig. 2C). By contrast, the $G\alpha_o$ protein GOA-1 reduces DAG abundance by triggering its phosphorylation by diacylglycerol kinase DGK-1 (*33*). Neuronal DAG primes both DCV and SV release via interaction with PKC-1(PKC-ε/η) (*34*) and UNC-13 (*35*), respectively. The bioamines and neuropeptides that are released from the DCVs can have both paracrine and autocrine activity (*36, 37*). This circuitry raised the possibility that Nementin-1-induced DCV release may initiate a positive feedback loop that amplifies DCV release and agonizes SV release as a secondary consequence (see green and yellow pathways in Fig. 2C).

We tested this hypothesis in three ways. First, we examined the impact of mutant components of the 'green' circuit depicted in Fig. 2C. We found that *egl-30* RF, which reduces DAG production, suppresses Nementin-1 convulsions (Fig. 3A). By contrast, *goa-1* RF and *dgk-1* loss-of-function (LF) mutants, which lack regulation of membrane DAG, enhance Nementin-1 convulsions. We also found that disruption of PKC-1 reduces Nementin-1 convulsions (Fig. 3A). Second, we asked whether the cell permeable DAG mimetic phorbol myristate acetate (PMA) enhances Nementin-1

convulsions and found that it did (Fig. 3A). PMA does not induce convulsions on its own, suggesting that PKC-1-agonism alone cannot severely disrupt motor activity. Finally, we asked whether Nementin-1's agonism of cholinergic signaling is dependent on the machinery needed for DCV release. Indeed, we found that the *unc-31(e169)* RF mutation and the *unc-43(n498)* GF mutation suppress Nementin-1's agonism of cholinergic signaling (Fig. 3C). Together, these observations are consistent with a model whereby Nementin-1 agonizes DCV release whose contents may stimulate autocrine/paracrine G-protein signaling, which in turn agonizes both more DCV release and cholinergic signaling.

Nementin Disrupts Parasitic Nematodes of Plants and Animals

We carried out a small structure-activity relationship (SAR) analysis of Nementin analogs assayed against free-living nematodes, parasitic nematodes, and non-target models (Table S2; Data S4). We purchased 18 commercially available analogs of Nementin-1 and found that Nementin-12 was the most potent inducer of acute motor phenotypes (Table S2). We expanded the SAR by synthesizing 22 analogs of Nementin-12 (see Materials and Methods). Nementins 1, 12-5, 13 and 14 demonstrated broad anthelmintic activity without inducing obvious phenotype against non-target organisms. In addition, Nementin analogs were identified with improved activity in each parasitic nematode model tested. These data suggest that the Nementin scaffold may be further refined to improve selectivity and potency.

Given that Nementin-1 synergistically enhances the activity of AChE inhibitors in *C. elegans*, we tested whether it might act similarly against parasitic nematodes. We tested Nementin-1's interaction with the organophosphate dichlorvos against *Strongyloides ratti*, a nematode parasite of mammals. Indeed, we find that Nementin-1 synergistically enhances dichlorvos' activity against *S. ratti* (Fig. 3E). Nementin-1 was also found to synthetically paralyze the plant-parasitic nematode *Meloidogyne hapla* with the carbamate AChE inhibitor oxamyl (Fig. 3F). Both dichlorvos and oxamyl are approved for field use (*38, 39*). The Nementins may therefore have added benefit against parasitic nematodes when used in combination with pesticides that are AChE inhibitors.

DISCUSSION

Here, we have developed a *C. elegans*-based pipeline to identify novel anthelmintic small molecules with phylum-selectivity. The pipeline was designed to yield broad-acting anthelmintics that acutely affect nematode behaviour. The strategy yielded four small molecules that exhibit phylum-selectivity within the limited range of organisms tested. We focused on one of these molecules, called Nementin-1, which induces *C. elegans* hyperactivity within seconds of exposure, followed by spastic convulsions minutes later. Several Nementin analogs affect parasitic nematodes from distinct clades at concentrations that fail to elicit obvious phenotypes from non-target organisms. Despite significant effort, we were not able to generate *C. elegans* mutants that resist the lethal effects of Nementin, suggesting that resistance in the wild may be difficult to achieve.

Our data support a model whereby Nementin exposure initiates DCV release, which in turn agonizes SV release that promotes cholinergic signaling. Nementin-induced convulsions depend on DCV release but not cholinergic signaling, indicating that agonized DCV release is key to Nementin's ability to disrupt motor behavior. How Nementin agonizes DCV release remains unclear. Despite the phenotypic similarities between Nementin exposure and *unc-43* RF mutants, our data suggests that Nementin is unlikely to inhibit UNC-43 in any canonical fashion. However, because of CaMKII's complexity and its many isoforms (*13, 40*), we cannot rule out the possibility that Nementin interacts with CaMKII in a complex and perhaps tissue-specific manner.

Nementin has several features that make it an attractive anthelmintic for further development. First, *in vitro* tests demonstrate that it exhibits potentially broad-spectrum activity while maintaining phylogenetic selectivity. Such a feature is key to the development of an environmentally safe anthelmintic. Second, Nementin analogs exhibit an *in vitro* potency that is comparable to several commercial anthelmintics. Third, the Nementin synthesis route is relatively simple and uses inexpensive starting materials ('Chemistry' in Supplementary Materials) (*41*). Finally, Nementin has the potential to reduce the amount of non-selective pesticides that are notoriously released into the environment.

Despite the toxicity concerns over indiscriminate activity, many AChE inhibitors such as trichlorfon, dichlorvos, coumaphos, aldicarb, fosthiazate, chlorpyrifos and oxamyl remain approved for nematicidal field use as of 2021 (*38*) (see the FDA Approved Animal Drug Products at https://tinyurl.com/by83ks98; and the US Environmental Protection Agency at https://tinyurl.com/3n3kf34n). Because of Nementin's nematode selectivity, combining Nementin with these AChE inhibitors has the potential to reduce the amount of pesticide applied while maintaining selectivity against the nematode parasites. Combining compounds that enhance acetylcholine release with AChE inhibitors is a novel strategy that may also prove effective in other pesticide contexts.

REFERENCES

1. M. Rashid *et al.*, A systematic review on modelling approaches for economic losses studies caused by parasites and their associated diseases in cattle. *Parasitology* **146**, 129-141 (2019).
2. S. Geerts, B. Gryseels, Drug resistance in human helminths: current situation and lessons from livestock. *Clin Microbiol Rev* **13**, 207-222 (2000).
3. D. J. Chitwood, Research on plant-parasitic nematode biology conducted by the United States Department of Agriculture-Agricultural Research Service. *Pest Manag Sci* **59**, 748-753 (2003).
4. U. N. D. o. E. a. S. Affairs, "Consolidated list of products whose consumption and / or sale have been banned, withdrawn, severely restricted or not approved by Governments," (New York, 2009).
5. H. C. Godfray, T. Garnett, Food security and sustainable intensification. *Philos Trans R Soc Lond B Biol Sci* **369**, 20120273 (2014).
6. M. B. Cole, M. A. Augustin, M. J. Robertson, J. M. Manners, The science of food security. *NPJ Sci Food* **2**, 14 (2018).
7. T. G. Geary, R. D. Klein, L. Vanover, J. W. Bowman, D. P. Thompson, The nervous systems of helminths as targets for drugs. *J Parasitol* **78**, 215-230 (1992).
8. L. Holden-Dye, R. J. Walker, Anthelmintic drugs and nematicides: studies in Caenorhabditis elegans. *WormBook*, 1-29 (2014).
9. A. R. Burns *et al.*, Caenorhabditis elegans is a useful model for anthelmintic discovery. *Nat Commun* **6**, 7485 (2015).

10. W. F. Schafer, Genetics of egg-laying in worms. *Annu Rev Genet* **40**, 487-509 (2006).

11. A. N. Somerville, SciFinder Scholar. *Journal of Chemical Education* **75**, 959-960 (1998).

12. S. Brenner, The genetics of Caenorhabditis elegans. *Genetics* **77**, 71-94 (1974).

13. D. J. Reiner, E. M. Newton, H. Tian, J. H. Thomas, Diverse behavioural defects caused by mutations in Caenorhabditis elegans unc-43 CaM kinase II. *Nature* **402**, 199-203 (1999).

14. A. Wei, T. Jegla, L. Salkoff, Eight potassium channel families revealed by the C. elegans genome project. *Neuropharmacology* **35**, 805-829 (1996).

15. I. P. de la Cruz, J. Z. Levin, C. Cummins, P. Anderson, H. R. Horvitz, sup-9, sup-10, and unc-93 may encode components of a two-pore K+ channel that coordinates muscle contraction in Caenorhabditis elegans. *J Neurosci* **23**, 9133-9145 (2003).

16. I. S. Greenwald, H. R. Horvitz, unc-93(e1500): A behavioral mutant of Caenorhabditis elegans that defines a gene with a wild-type null phenotype. *Genetics* **96**, 147-164 (1980).

17. Y. C. Huang *et al.*, Gain-of-function mutations in the UNC-2/CaV2alpha channel lead to excitation-dominant synaptic transmission in Caenorhabditis elegans. *Elife* **8**, (2019).

18. M. Jospin *et al.*, A neuronal acetylcholine receptor regulates the balance of muscle excitation and inhibition in Caenorhabditis elegans. *PLoS Biol* **7**, e1000265 (2009).

19. L. Salkoff *et al.*, Potassium channels in C. elegans. *WormBook*, 1-15 (2005).

20. M. Kasap, D. S. Dwyer, Clozapine, nimodipine and endosulfan differentially suppress behavioral defects caused by gain-of-function mutations in a two-pore domain K(+) channel (UNC-58). *Neurosci Res*, (2020).

21. C. M. Hoover *et al.*, A novel CaM kinase II pathway controls the location of neuropeptide release from Caenorhabditis elegans motor neurons. *Genetics* **196**, 745-765 (2014).

22. S. Speese *et al.*, UNC-31 (CAPS) is required for dense-core vesicle but not synaptic vesicle exocytosis in Caenorhabditis elegans. *J Neurosci* **27**, 6150-6162 (2007).

23. M. Hammarlund, S. Watanabe, K. Schuske, E. M. Jorgensen, CAPS and syntaxin dock dense core vesicles to the plasma membrane in neurons. *J Cell Biol* **180**, 483-491 (2008).

24. P. Laurent *et al.*, Genetic dissection of neuropeptide cell biology at high and low activity in a defined sensory neuron. *Proc Natl Acad Sci U S A* **115**, E6890-E6899 (2018).

25. M. R. Lackner, S. J. Nurrish, J. M. Kaplan, Facilitation of synaptic transmission by EGL-30 Gqalpha and EGL-8 PLCbeta: DAG binding to UNC-13 is required to stimulate acetylcholine release. *Neuron* **24**, 335-346 (1999).

26. A. Alfonso, K. Grundahl, J. S. Duerr, H. P. Han, J. B. Rand, The Caenorhabditis elegans unc-17 gene: a putative vesicular acetylcholine transporter. *Science* **261**, 617-619 (1993).

27. M. Nguyen, A. Alfonso, C. D. Johnson, J. B. Rand, Caenorhabditis elegans mutants resistant to inhibitors of acetylcholinesterase. *Genetics* **140**, 527-535 (1995).

28. C. Cambon, C. Declume, R. Derache, Effect of the insecticidal carbamate derivatives (carbofuran, pirimicarb, aldicarb) on the activity of acetylcholinesterase in tissues from pregnant rats and fetuses. *Toxicol Appl Pharmacol* **49**, 203-208 (1979).

29. A. Ianevski, A. K. Giri, T. Aittokallio, SynergyFinder 2.0: visual analytics of multi-drug combination synergies. *Nucleic Acids Res* **48**, W488-W493 (2020).

30. G. Yadav, S. Ganguly, Structure activity relationship (SAR) study of benzimidazole scaffold for different biological activities: A mini-review. *Eur J Med Chem* **97**, 419-443 (2015).

31. M. R. Koelle, Neurotransmitter signaling through heterotrimeric G proteins: insights from studies in C. elegans. *WormBook* **2018**, 1-52 (2018).

32. M. Robatzek, J. H. Thomas, Calcium/calmodulin-dependent protein kinase II regulates Caenorhabditis elegans locomotion in concert with a G(o)/G(q) signaling network. *Genetics* **156**, 1069-1082 (2000).

33. K. G. Miller, M. D. Emerson, J. B. Rand, Goalpha and diacylglycerol kinase negatively regulate the Gqalpha pathway in C. elegans. *Neuron* **24**, 323-333 (1999).

34. D. Sieburth, J. M. Madison, J. M. Kaplan, PKC-1 regulates secretion of neuropeptides. *Nat Neurosci* **10**, 49-57 (2007).

35. J. E. Richmond, W. S. Davis, E. M. Jorgensen, UNC-13 is required for synaptic vesicle fusion in C. elegans. *Nat Neurosci* **2**, 959-964 (1999).

36. W. Steuer Costa, S. C. Yu, J. F. Liewald, A. Gottschalk, Fast cAMP Modulation of Neurotransmission via Neuropeptide Signals and Vesicle Loading. *Curr Biol* **27**, 495-507 (2017).

37. T. M. Stawicki, S. Takayanagi-Kiya, K. Zhou, Y. Jin, Neuropeptides function in a homeostatic manner to modulate excitation-inhibition imbalance in C. elegans. *PLoS Genet* **9**, e1003472 (2013).

38. S. A. Nixon *et al.*, Where are all the anthelmintics? Challenges and opportunities on the path to new anthelmintics. *Int J Parasitol Drugs Drug Resist* **14**, 8-16 (2020).

39. M. Abdel-Sattar, A. M. Haikal, S. E. Hammad, Meloidogyne incognita population control and nutritional status and productivity of Thompson seedless grapevines managed with different treatments. *PLoS One* **15**, e0239993 (2020).

40. J. B. Myers *et al.*, The CaMKII holoenzyme structure in activation-competent conformations. *Nat Commun* **8**, 15742 (2017).

41. P. Ertl, A. Schuffenhauer, Estimation of synthetic accessibility score of drug-like molecules based on molecular complexity and fragment contributions. *J Cheminform* **1**, 8 (2009).

42. D. Kulke *et al.*, In vitro efficacy of cyclooctadepsipepdtides and aminophenylamidines alone and in combination against third-stage larvae and adult worms of Nippostrongylus brasiliensis and first-stage larvae of Trichinella spiralis. *Parasitol Res* **112**, 335-345 (2013).

43. E. B. Rapson, D. L. Lee, S. D. Watts, Changes in the acetylcholinesterase activity of the nematode Nippostrongylus brasiliensis following treatment with benzimidazoles in vivo. *Mol Biochem Parasitol* **4**, 9-15 (1981).

44. A. M. Lumley, D. L. Lee, Nippostrongylus brasiliensis and Nematodirus battus: changes in numbers and weight during the course of infection. *Exp Parasitol* **52**, 183-190 (1981).

45. W. K. Huang *et al.*, Mutations in Acetylcholinesterase2 (ace2) increase the insensitivity of acetylcholinesterase to fosthiazate in the root-knot nematode Meloidogyne incognita. *Sci Rep* **6**, 38102 (2016).

46. J. R. Volpatti *et al.*, Identification of drug modifiers for RYR1-related myopathy using a multi-species discovery pipeline. *Elife* **9**, (2020).

47. C. Liu, Zhang, Y., Liu, N. and Qiu, J., A simple and efficient approach for the palladium-catalyzed ligand-freeSuzuki reaction in water. *Green Chemistry* **14**, 4 (2012).

48. Y. Geng *et al.*, O-Difluorodeuteromethylation of phenols using difluorocarbene precursors and deuterium oxide. *Org Biomol Chem* **16**, 1807-1811 (2018).

49. M. Ando, T. Wada, N. Sato, Facile one-pot synthesis of N-difluoromethyl-2-pyridone derivatives. *Org Lett* **8**, 3805-3808 (2006).

50. M. D. Squire *et al.*, Molecular cloning and functional co-expression of a Caenorhabditis elegans nicotinic acetylcholine receptor subunit (acr-2). *Recept Channels* **3**, 107-115 (1995).

51. H. A. Petrash, A. Philbrook, M. Haburcak, B. Barbagallo, M. M. Francis, ACR-12 ionotropic acetylcholine receptor complexes regulate inhibitory motor neuron activity in Caenorhabditis elegans. *J Neurosci* **33**, 5524-5532 (2013).

52. W. R. Schafer, C. J. Kenyon, A calcium-channel homologue required for adaptation to dopamine and serotonin in Caenorhabditis elegans. *Nature* **375**, 73-78 (1995).

53. E. A. Mathews *et al.*, Critical residues of the Caenorhabditis elegans unc-2 voltage-gated calcium channel that affect behavioral and physiological properties. *J Neurosci* **23**, 6537-6545 (2003).

54. S. Brenner, The Genetics of Caenorhabditis elegans. *Genetics* **77**, 71-94 (1974).

55. J. Z. Levin, H. R. Horvitz, Three new classes of mutations in the Caenorhabditis elegans muscle gene sup-9. *Genetics* **135**, 53-70 (1993).

56. M. T. Kunkel, D. B. Johnstone, J. H. Thomas, L. Salkoff, Mutants of a temperature-sensitive two-P domain potassium channel. *J Neurosci* **20**, 7517-7524 (2000).

Acknowledgements:

We are grateful for the strains given to us by the *Caenorhabditis* Genetics Center (University of Minnesota), Marie-Anne Félix (IBENS, Paris), Ken Miller (Oklahoma Medical Research Foundation), and Mei Zhen and Wesley Hung (Lunenfeld-Tanenbaum Research Institute, Toronto). Many thanks to Dr. Doug Colwell and Dawn Gray at the Lethbridge and Agri-Food Canada Research Centre for supplying faeces from infected calves for *Cooperia oncophora* egg collection.

Funding:

Research in the I.Z. lab is partially supported by the United States Department of Agriculture, Agricultural Research Service. P.J.R. is supported by CIHR project grants (313296 and 173448). P.J.R. is a Canada Research Chair (Tier 1) in Chemical Genetics.

Author Contributions

Conceptualization: PJR, SH

Methodology: SH, JJK, K-L C, AA, MK, CH, JP, JRV, MG, JS, VW, BMP, EMR, ASV,

Investigation: SH, JJK, AB, MK, CH, JP, C'DA, Y-H K, JRV, MG, JS, VW, BMP, EMR, ADS

Visualization: PJR, SH

Funding acquisition: PJR

Project administration: PJR

Supervision: PJR, JG, IS, SRC, JJD, CMY, JK, IZ, ML

Writing – original draft: PJR, SH, JJK, K-LC, AA, SRC, DK, JK

Writing – review & editing: PJR, SH, AB, JJK, SC, DK, JK, IZ, ML

Competing interests:

Mention of trade names or commercial products in this publication is solely for the purpose of providing specific information and does not imply recommendation or endorsement by the U.S. Department of Agriculture. USDA is an equal opportunity provider and employer. S.H., J.K., A.R.B., K-L.C., J.P., M.L. and P.J.R. have patents pending related to Nementin.

Data and materials availability:

Original data for all analyses presented are included in Data S1-S4. Original images for analyses can be made available per request through the corresponding author P.J.R.

Supplementary Materials

Supplementary Text

Materials and Methods

Figs. S1 to S6

Table S1

References 42-56

Movies S1 to S6

Data S1 to S4

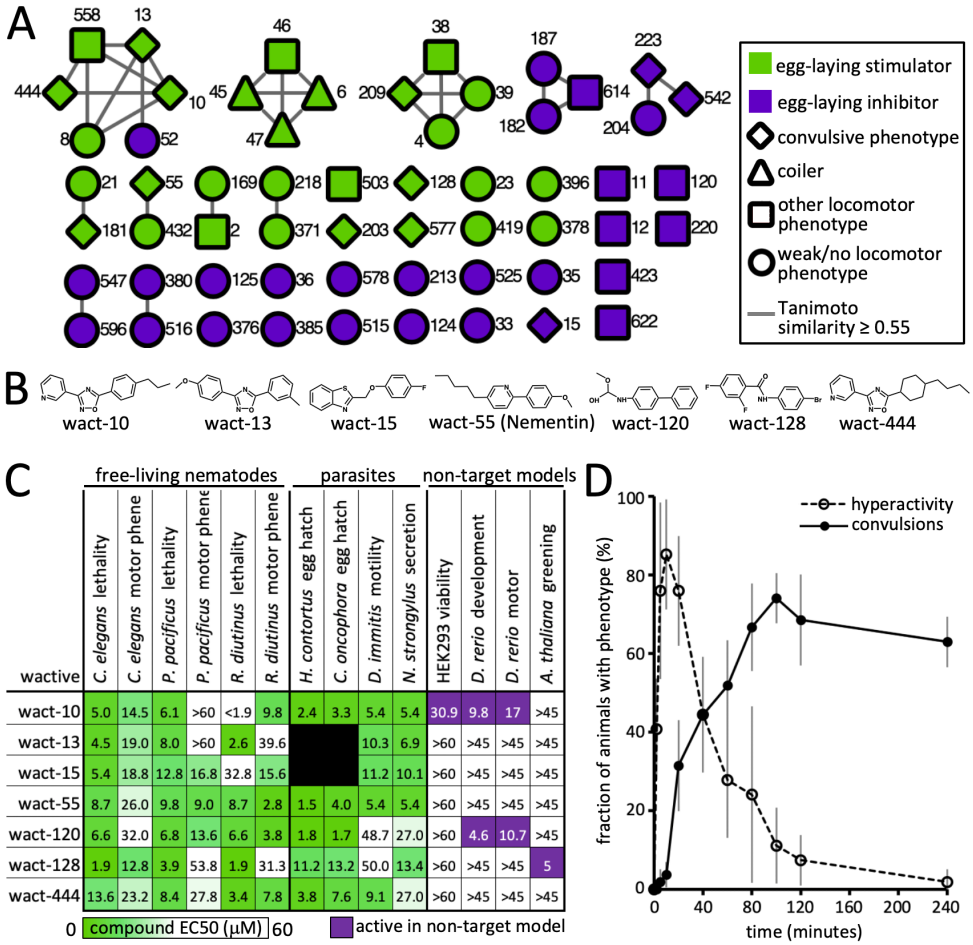

Fig. 1. A motor-centric pipeline yields convulsing-inducing Nementin-1. (**A**) A structure similarity network of the 58 egg-laying modulators. Each node represents a numbered wactive molecule. Connecting lines indicate shared structural similarity. Additional information is provided in Table 1. (**B**) Structures of the 7 prioritized neuromodulators. (**C**) Bioactivity of the seven prioritized molecules. Data are EC50s except for the *A. thaliana* greening assay, which is the lowest concentration that yields a discernible difference from control. (**D**) A time-course analysis of 60 μM Nementin-1-induced locomotory phenotypes. Data are the mean of biological triplicate measurement of 18 animals per each time point. The standard deviation is shown.

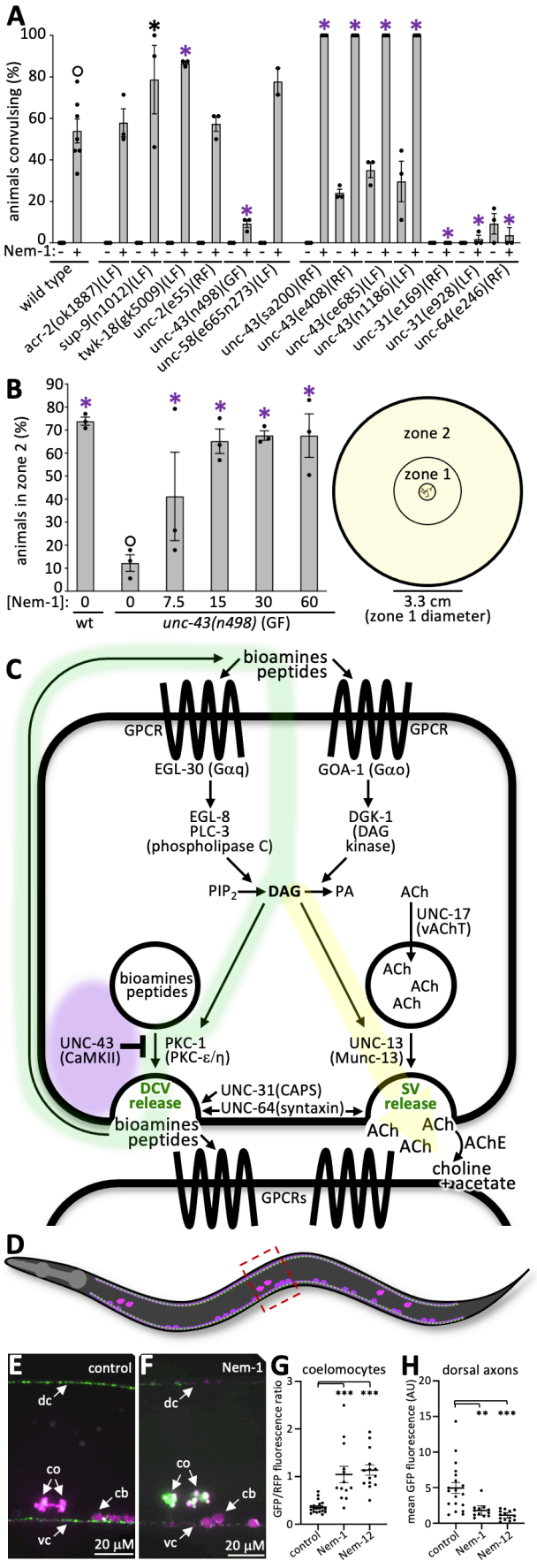
A
animals convulsing (%)
Nem-1:
wild type
acr-2(ok1887)(LF)
sup-9(n1012)(LF)
twk-18(gk5009)(LF)
unc-2(e55)(RF)
unc-43(n498)(GF)
unc-58(e665n273)(LF)
unc-43(sa200)(RF)
unc-43(e408)(RF)
unc-43(ce685)(LF)
unc-43(n1186)(LF)
unc-31(e169)(RF)
unc-31(e928)(LF)
unc-64(e246)(RF)
B
animals in zone 2 (%)
[Nem-1]: 0 0 7.5 15 30 60
wt
unc-43(n498) (GF)
zone 2
zone 1
3.3 cm
(zone 1 diameter)
C
bioamines
peptides
GPCR
GPCR
EGL-30 (Gαq)
GOA-1 (Gαo)
EGL-8
PLC-3
(phospholipase C)
DGK-1
(DAG
kinase)
PIP2
DAG
PA
ACh
UNC-17
(vAChT)
bioamines
peptides
ACh
ACh
ACh
UNC-43
(CaMKII)
PKC-1
(PKC-ε/η)
UNC-13
(Munc-13)
DCV
release
UNC-31(CAPS)
UNC-64(syntaxin)
SV
release
bioamines
peptides
ACh
ACh
ACh
AChE
choline
+acetate
GPCRs
D
E
control
dc
co
cb
vc
20 μM
F
Nem-1
dc
co
cb
vc
20 μM
G
coelomocytes
GFP/RFP fluorescence ratio
control
Nem-1
Nem-12
H
dorsal axons
mean GFP fluorescence (AU)
control
Nem-1
Nem-12

Fig. 2. Nementin agonizes dense core vesicle release. (**A**) Convulsions induced by Nementin-1 (Nem-1) (60 μM) in the indicated genetic background after 80 minutes. The mean of three biological replicates with 18 animals per trial is shown. (**B**) The mean percentage of animals of the indicated genotype (three trials with ~150 animals per trial) that locomote to zone 2 over 180 minutes after being placed in the centre of a plate (see schematic on right). For A and B, black and purple asterisks represent $p<0.05$ and $p<0.001$, Chi-square test of independence with Bonferroni correction relative to control (open circle); the standard error of the mean (SEM) is shown. (**C**) A schematic of neuronal signaling pathways relevant to Nementin activity. Purple glow indicates area of possible Nementin action; the green glow indicates how DCV neurotransmitter cargo may activate $G\alpha_q$ and $G\alpha_o$ signaling pathways; the yellow glow indicates how the secondary messenger diacylglycerol (DAG) can also promote synaptic vesicle release. (**D**) Schematic of adult (strain KG4247) expressing INS-22::GFP (green dots; packaged into DCVs) and secreted mCherry (fuchsia) in cholinergic motor neurons (cell bodies are oval). mCherry is constitutively secreted and taken up by the coelomocytes (three pairs of pink objects in the animal). Box indicates the area shown in E and F. Anterior is the left and dorsal is up. (**E** and **F**) Images of the midbody region of control and 60 µM Nementin-1-treated KG4247 animals after 4 hours. dc, dorsal cord; vc, ventral cord; co, coelomocytes; cb, cell bodies. (**G**) Quantification of the midbody coelomocytes (ratio of measured GFP/RFP) and dorsal cord fluorescence (relative to background tissues) of the animal. AU, arbitrary units., 1-way ANOVA with Dunnett correction for multiple

comparisons; ** $p<0.01$; *** $p<0.001$; SEM is shown. Other regions of the animal are quantified in Fig. S4.

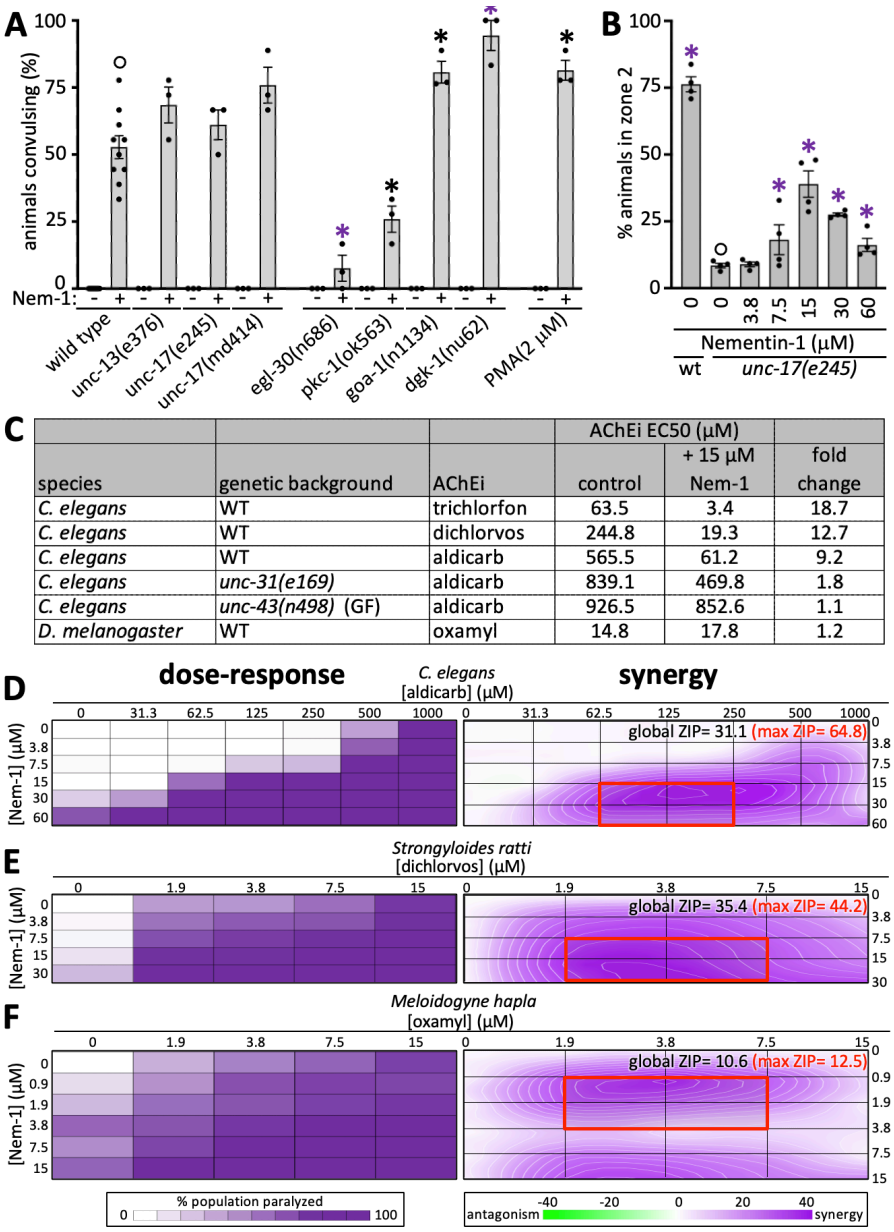

Fig. 3. Nementin enhances AChE inhibitor activity via agonism of DCV release. (**A**) Convulsions induced after 80 minutes of exposure to Nementin-1 (Nem-1) (60 *μ*M) or vehicle control in the background of the indicated mutant gene, or in the background of 24 hours of preincubation with the DAG memetic PMA. (**B**) The ability of wild type (WT) or *unc-17* mutant animals to productively locomote to zone 2 over 180 minutes after being placed in the centre of a plate (see schematic in Fig. 2B) in the indicated

Nementin concentration. For both A and B, black asterisk $p<0.01$, purple asterisk $p<0.001$, Bonferroni corrected Chi-square test of independence relative to control (open circle); SEM is shown. (**C**) Acetylcholinesterase inhibitor (AChEi) EC50s for different species and genetic backgrounds. Oxamyl is the only AChEi tested that exhibited activity against flies. Data are the mean of 3 biological replicates scoring 18 animals per condition. (**D-F**) On the left are double dose-response analyses of Nementin-1 (y-axis) vs the indicated AChEi (x-axis) in the indicated nematode species. On the right are the corresponding zero interaction potency (ZIP) synergy score heatmaps for the intersection of the indicated compound concentrations. The legends at the bottom respectively apply to charts above them. The area of max ZIP score is indicated with a red box and the global and max ZIP δ-scores are indicated. N=3 trials for *elegans* with n=18 within each trial, N=6 trials for *ratti* with $n \geq 30$ within each trial, $N \geq 3$ trials for *hapla* with $n \geq 15$ within each trial.

				locomotor phenotype[c]							larval lethal assay[d]						
	wactive	Chembridge ID[a]	egg-laying phenotype[b]	shrinker	shaker	coiler	jerky-Unc	reversal-defective	paralyzed	slow	*C. elegans*	*C. briggsae*	*P. pacificus*	*C. oncophora*	*H. contortus*	HEK293T[e]	*Danio rerio*[f]
Convulsive (primarily)																	
1	wact-10	5905384	Egl-S	30	60	n	n	n	n	n	8	30	30	4	60	n	n
2	wact-13	7632721	Egl-S	30	n	n	30	60	n	n	8	30	30	8	60	n	n
3	wact-15	7687977	Egl-I	30	n	n	30	30	n	n	8	60	60	8	60	n	n
4	wact-55	5688274	Egl-S	60	60	n	n	n	30	n	8	30	30	8	8	n	n
5	wact-128	7971816	Egl-S	30	n	n	n	n	n	n	30	30	30	4	60	n	n
6	wact-181	9032631	Egl-S	30	>60	n	n	n	n	n	30	30	8	15	60	30	dead
7	wact-209	7153658	Egl-S	30	60	n	n	n	n	n	30	30	30	15	60	60	n
8	wact-223	7638283	Egl-I	60	n	n	n	n	n	n	n	n	n	60	60	60	n
9	wact-542	7781713	Egl-I	30	n	n	n	n	n	n	n	n	60	15	60	n	dev
Shaker (primarily)																	
10	wact-203	9062286	Egl-S	>60	60	n	60	n	n	n	30	30	30	15	60	n	dev
11	wact-444	5910902	Egl-S	n	30	n	n	n	n	n	30	30	30	15	60	n	n
12	wact-577	9039023	Egl-S	n	60	n	n	n	60	n	60	60	60	60	60	n	n
Coiler (primarily)																	
13	wact-6	5419367	Egl-S	n	n	30	n	n	30	n	30	30	30	>60	>60	30	card
14	wact-45	5426270	Egl-S	n	n	30	60	n	60	n	n	n	n	60	>60	n	n
15	wact-47	5427063	Egl-S	n	n	60	>60	n	>60	n	30	n	n	60	>60	30	card
Reversal Defective (primarily)																	
16	wact-38	5356411	Egl-S	n	n	n	n	30	n	n	30	30	30	8	60	n	n
17	wact-558	9008591	Egl-S	n	n	n	n	60	n	30	8	30	30	60	60	n	n
Jerky-Unc (primarily)																	
18	wact-46	5426998	Egl-S	n	n	n	30	n	>60	n	n	60	n	8	>60	n	card
19	wact-120	7889289	Egl-I	n	n	n	60	n	n	n	30	30	30	4	60	n	n
Paralysis																	
20	wact-11	6222549	Egl-I	n	n	n	n	n	30	n	8	8	8	8	60	n	n
21	wact-12	7003409	Egl-I	n	n	n	n	n	n	n	8	30	8	8	60	n	n
22	wact-220	5784085	Egl-I	n	n	n	n	n	30	n	8	n	30	>60	60	n	dev
Slow																	
23	wact-423	5547023	Egl-I	n	n	n	n	n	n	30	60	n	60	8	60	30	n
24	wact-503	7568929	Egl-S	n	n	n	n	n	n	30	60	60	60	60	60	30	n
25	wact-614	9039813	Egl-I	n	n	n	n	n	n	30	8	30	60	>60	>60	30	dead
26	wact-622	5373894	Egl-I	n	n	n	n	n	n	30	n	n	n	60	>60	30	n
Weak or No Locomotory Phenotype																	
27	wact-2	5185411	Egl-S	n	n	n	n	n	n	60	8	8	8	8	>60	60	dev
28	wact-4	5352487	Egl-S	>60	n	n	n	n	n	n	30	30	30	30	60	n	n
29	wact-8	5652977	Egl-S	n	n	n	n	>60	n	n	30	8	8	60	>60	30	dead
30	wact-21	5129511	Egl-S	n	n	n	>60	n	n	n	30	n	n	8	60	n	n
31	wact-23	5156707	Egl-S	n	n	n	n	>60	n	n	30	30	8	8	60	30	dead
32	wact-33	5308651	Egl-I	n	n	n	n	n	n	n	30	30	30	8	>60	30	n
33	wact-35	5344384	Egl-I	n	n	n	n	60	n	n	30	60	60	8	60	30	n
34	wact-36	5347942	Egl-I	n	n	n	n	n	n	n	n	n	n	8	60	n	n
35	wact-39	5357418	Egl-S	n	n	n	n	n	n	n	30	n	30	8	60	n	n
36	wact-62	6269333	Egl-I	depleted							30	30	60	8	60	n	n
37	wact-124	7943845	Egl-I	n	n	n	n	n	n	>60	30	30	30	8	60	60	card
38	wact-125	7949759	Egl-I	n	n	n	n	n	n	n	30	60	8	60	>60	n	n
39	wact-169	9024879	Egl-S	n	n	n	n	n	n	n	8	30	8	>60	>60	n	n
40	wact-182	9033974	Egl-I	n	n	n	n	60	n	n	30	60	n	n	n	60	n
41	wact-187	9035461	Egl-I	n	n	n	n	n	n	n	<<30	60	n	n	n	60	n
42	wact-204	9063096	Egl-I	n	n	n	n	>60	n	n	30	60	30	>>60	>60	30	dead
43	wact-213	5107544	Egl-I	n	n	n	n	n	n	n	60	n	n	>60	>60	n	n
44	wact-218	5379978	Egl-S	n	n	n	>60	n	n	n	8	30	30	15	60	30	n
45	wact-371	5100784	Egl-S	n	n	n	n	n	n	n	8	60	60	8	60	30	n
46	wact-376	5192203	Egl-I	depleted							60	30	30	8	60	n	dead
47	wact-378	5192696	Egl-S	n	n	n	n	n	n	60	30	60	60	8	60	n	n
48	wact-380	5218876	Egl-I	n	n	n	n	n	n	n	n	n	30	>60	n	n	card
49	wact-385	5238652	Egl-I	n	n	n	n	>60	n	n	30	60	60	8	60	30	dead
50	wact-396	5322542	Egl-S	n	n	n	n	n	n	n	60	60	60	8	60	n	n
51	wact-419	5469460	Egl-S	>60	>60	n	n	n	n	n	60	60	60	60	60	n	n
52	wact-432	5689365	Egl-S	n	n	n	n	n	n	n	60	60	60	8	60	n	n
53	wact-515	7653692	Egl-I	n	n	n	n	>60	n	n	n	n	60	60	60	30	n
54	wact-516	7664300	Egl-I	>60	n	n	n	n	n	n	>60	60	30	4	60	n	card
55	wact-525	7705966	Egl-I	n	n	n	n	n	n	n	n	n	n	60	60	60	n
56	wact-547	7877602	Egl-I	n	n	n	n	n	n	n	n	n	60	>60	>60	30	dead
57	wact-578	9040453	Egl-I	n	n	n	n	n	n	n	30	n	n	8	8	n	dead
58	wact-596	5649594	Egl-I	n	n	n	n	n	n	n	30	30	30	>60	60	n	dead

Table 1. *C. elegans* locomotor phenotype and phylogenetic activity profile of identified egg-laying modulators.

[a]The Chembridge Inc. identification (ID) numbers are indicated.

[b]Egg-laying phenotype; Egl-S = egg-laying stimulators; Egl-I = egg-laying inhibitors.

[c]The observed acute motor phenotypes are indicated. The concentration at which strong and moderate phenotypes appear are indicated in bright green. The concentration at which weaker phenotypes appear are indicated in light gray. 'n' indicates no phenotype was observed.

[d]Larval lethality phenotypes; the previously reported results (*9*) of liquid-based larval lethal assays (for *C. elegans*, *C. briggsae*, and *P. pacificus*) are shown. The lowest concentration at which 100% of the larvae die/arrest is shown. Colours highlight relatively potent activity.

[e]HEK293T cell proliferation summary; compounds that reduce HEK293T proliferation below one standard of deviation from the mean at 30 or 60 μM as previously reported are indicated as purple '30' or '60', respectively (see (*9*) for details).

[f]*Danio rerio* (zebrafish) developmental defect summary; molecules that induce cardiac defects (card), developmental defects (dev) or death (dead) at a concentration of 10 μM as previously reported (*9*) are summarized here. Throughout the table, 'n' reports no lethality or phenotype observed.

Supplementary Materials for

A Nematode-Selective Potentiator of Organophosphate and Carbamate Agrochemicals

Sean Harrington, Jessica J. Knox, Andrew R. Burns, Ken-Loon Choo, Aaron Au, Megan Kitner, Cecile Haeberli, Jacob Pyche, Cassandra D'Amata, Yong-Hyun Kim, Jonathan R. Volpatti, Maximillano Guiliani, Jamie Snider, Victoria Wong, Bruna M. Palmeira, Elizabeth M. Redman, Aditya S. Vaidya, John Gilleard, Igor Stagljar, Sean R. Cutler, Daniel Kulke, James J. Dowling, Christopher M. Yip, Jennifer Keiser, Inga Zasada, Mark Lautens, and Peter J. Roy*

*Correspondence to: peter.roy@utoronto.ca

This PDF file includes:

Supplementary Text
Ethics Statement
Materials and Methods
Figs. S1 to S6
Table S1 and S2
Captions for Movies S1 to S6
Captions for Data S1 to S4
References

Other Supplementary Materials for this manuscript include the following:

Movies S1 to S6

Data S1. Egg-laying rates with and without a stimulatory cocktail.

Data S2. The Wactive Library egg-laying screen data.

Data S3. The locomotory survey of the egl-modulators.

Data S4. Nematode and Counter-Screen Bioassay Data.

Supplementary Text

To identify egg-laying stimulators, we screened small molecules in the background of M9 worm buffer (*1*). Animals incubated in M9-vehicle control wells lay 1.1 eggs per hour on average (Fig. S1C-D; Data S1). To identify egg-laying inhibitors, we screened small molecules in the background of exogenous serotonin plus nicotine that stimulates animals to lay an average of 7.5 eggs per hour (see methods; Fig. S1C-D; Data S1).

We cross-referenced the list of 58 acute egg-laying modulators to the list of 247 wactive molecules that are lethal in six-day viability assays (*1*). We found a 1.8-fold enrichment of lethality among the stimulators ($p<0.001$) (Fig. S1F), suggesting that excessive neuromuscular modulation may lead to death. A 1.4-fold enrichment of lethality among the inhibitors was also found ($p<0.05$), which is not unexpected given that egg-laying inhibition is certain to be a consequence of molecules that kill rapidly.

Ethics Statement

55 DK: Experiments on *D. immitis* and *N. brasiliensis* were performed in the laboratories of Bayer Animal Health GmbH (Monheim, Germany) in accordance with the local Animal Care and Use Committee and governmental authorities. JK: The generation of *N. americanis*, *T. muris*, S. ratti, and *H. polygyrus* and in vitro studies were carried out at the Swiss Tropical Institute (Basel, Switzerland), in accordance with both cantonal

60 (license no. 2070) and Swiss national regulations on animal experimentation. JD: All zebrafish experiments were performed in compliance with any relevant ethical regulations, specifically following an institutionally reviewed and approved animal use protocol as well as the policies and guidelines of the Canadian Council on Animal Care and Animals for Research Act of Ontario.

65

Materials and Methods

Free-Living Nematode Strains and Culture

All nematode strains were cultured using standard methods at 20 °C unless otherwise indicated (*2*). The N2 (wild-type) strain of *Caenorhabditis elegans, Caenorhabditis briggsae* strain AF16 and *Pristionchus pacificus* strain PS312 were all obtained from the *C. elegans* Genetic Center (CGC; University of Minnesota). *Rhabditophanes sp. KR3021* was obtained from Marie-Anne Félix (Institute of Biology of the Ecole Normale Supérieure (IBENS), Paris, France). Mutant *C. elegans* strains were also obtained from the *C. elegans* Genetic Center.

C. elegans Small Molecule Screens and Phenotypic Analyses

A library of 486 small-molecules (Chembridge) previously found to induce phenotypes in *C. elegans* (486 worm actives, aka wactives; 26108372) were tested for their ability to modulate *C. elegans* egg-laying. Drug dilutions were prepared from stock plates using a 96-well pinner tool (FP3S200 V&P Scientific, Inc.) transferring 0.3 mL of drug stock solution prepared in DMSO.

C. elegans Egg-laying Assay

To screen for small molecules that modulate egg laying, ~20 young-adult wild-type (N2 Bristol) animals were pipetted in 15 mL of M9 buffer to 96-well flat-bottom polystyrene plates (2024-06 TC plate – Sarstedt) to a final volume of 50 mL containing 60 µM of test

molecules in either 1) M9 buffer to identify egg-laying stimulators; or 2) a combination of 12.3 mM serotonin creatine sulfate monohydrate (H775 - Sigma-Aldrich) and 7.7 mM nicotine (N3876 - Sigma-Aldrich) in M9 buffer that induces a robust egg-laying response to identify egg-laying inhibitors (aka NS condition). Screen molecules were transferred to test wells using a 96-well pinner tool (FP3S200 V&P Scientific, Inc.) transferring 0.3 mL of drug stock solution prepared in DMSO. Plates were incubated for 1 hour at room-temperature. After 1 hour 182 mL of solution containing 50mM sodium azide (71289 – Sigma Aldrich) and 0.25% sodium dodecyl sulfate (SDS001.100 - BioShop) in M9 buffer using a multi-channel pipette followed by 182 mL of M9 buffer to raise the volume of each well such that a flat meniscus is produced. Plates were immediately imaged on the *2020 Imager* and were separated by 5 minutes to allow time for preparation of subsequent plates for imaging. After imaging egg-laying data was extracted from raw captured images using the 'Egg & Worm Counter' ImageJ plugin described above. Stimulators were considered molecules that stimulated egg-laying ≥ 2-fold greater than two proximal controls in the benign M9 buffer conditions with significance ($p < 0.05$ unpaired heteroscedastic t-test) over triplicate measurement (3 test compared against 6 control wells). Egl inhibitors were considered molecules that suppressed egg-laying ≤ 0.5 the normalized egg-laying rate of proximal controls in the 'nicotine (7.7 mM) + serotonin (12.3 mM)' condition described above with significance ($p < 0.05$ unpaired heteroscedastic t-test) over triplicate measurement (3 test compared against 6 control wells). Primary egg-laying modulators that reached the above threshold in at least 1 of 2 additional tests were considered bonafide 'Egl modulators'. As a more stringent criteria

to narrow our focus on robust Egl modulators we limited our inquiry of Egl stimulators that induced Egl ≥ 2 fold that of control over 3 trials (primary screen + 2 retests) or stimulated Egl 3-fold relative to control over at least 2 of 3 trials and Egl inhibitors that suppressed Egl ≤ 2 fold control over all 3 re-tests or molecules that suppressed Egl ≤ 3 fold that of control in at least 2 of 3 trials.

Construction of the '2020 Imager'

High-content brightfield data were acquired on a custom brightfield 96 well-plate imager. The well-plate was mounted on a stationary platform, while the imaging setup travelled parallel to the bottom of the well-plate via a motorized stage. The plate was illuminated from above using a 10 W white LED. Underneath the plate, an Olympus 4x objective (Olympus, UPLFLN4XPH) was used with a 150 mm tube lens (Thorlabs, AC254-150-A-ML) to create an effective magnification of 3.33x. A mirror was used to maintain a low-profile imaging setup and minimize distortions induced by the displacement of the imaging optics. The magnified image was projected onto a 4K line scan camera (Dalsa, P2-23-04K40), resulting in an effective resolution of 3.00 μm/px. The camera had a single line of 4096 px which captured an area of 12.3mm by 3 μm with a bit depth of 10 bits. To capture a row of 12 wells, the image acquisition software (EPIX Inc, XCAP-Ltd) was setup to acquire scans at 3000 lines/s. This resulted in a 4K by 48K image that was acquired in about 15 seconds. To sequentially image each row in of a well-plate, an Arduino UNO was used to synchronize the image acquisition with the movement of the motorized stage. For additional details see Aaron Au's Master's thesis titled: 'Optical

Imaging Strategies for High-Content Studies of Development' available through the URL https://tspace.library.utoronto.ca/bitstream/1807/91538/3/Au_Aaron_K_201811_MAS_thesis.pdf.

135 ImageJ Analysis of *C. elegans* Egg-Laying Rate

A custom ImageJ (version 1.52i) plugin was used to quantify the number of worms and eggs present in each well (versions used available on github: github.com/seanph16/WormScanner3000/upload). Prior to object counting a threshold was applied based on the mean pixel intensity in each well image. The number of
140 worms in a well was determined by measuring the area covered by non-egg shaped objects divided by the average area of a worm. Worm-like objects were recognized by the built-in ImageJ analyze particles function identifying objects greater than 11450 px in area with a circularity of 0.029–0.80 (the approximate minimum single adult worm size and range of shape circularities adopted by a worm) divided by the median worm
145 area. Single eggs were counted by first creating a mask of egg and egg clump shaped objects (objects that are 300-6000 px in area with circularity of 0.15-1.00), applying the built-in ImageJ 'Watershed' function to recognize single eggs within clumps and counting objects with a circularity of 0.5–1 with a size of 300-2500 px. The number of egg objects divided by the number of worms was used as a read-out of egg-laying
150 behaviour.

C. elegans Locomotory Survey

Locomotor phenotype analyses were done in 24-well plates with 1 mL of MYOB substrate (27.5 g Trizma HCl, 12 g Trizma Base, 230 g bacto tryptone, 10 g NaCl, 0.4 g cholesterol (95%)) seeded with 25 μL of OP50 *Escherichia coli* on each well. Each compound was added to the MYOB substrate before pouring to achieve the desired final concentrations of 30 μM or 60 μM after diffusion through the media. The final concentration of dimethyl sulfoxide (DMSO) in each of the wells was 1% v/v. Young adult or late fourth-staged larval worms are transferred into each well using a platinum wire pick. A Leica MZ75 stereomicroscope was used to visualize the movement of worms on the solid substrate. The specific locomotor phenotype (i.e. 'rubber-band' or 'coiler') was noted, and a qualitative assessment of the severity was made based on the degree of locomotor incapacitation and penetrance of the phenotype. Samples deemed 'Severe' indicated a strong perturbation and high penetrance, 'moderate' indicated a strong phenotype with low penetrance or a weak phenotype that is highly penetrant, and 'mild' indicated a weak phenotype that has low penetrance. Paralysis was distinguished from death by the presence of pharyngeal pumping.

C. elegans Motor Phenotype Analyses: The intensity of nementin-induced convulsions is tightly correlated with the degree of paralysis (i.e. animals that exhibit paralysis invariably convulse). We therefore used the degree of paralysis as a conveniently measurable proxy of convulsion intensity. In our survey of the effects of nementin analogs across *C. elegans, P. pacificus* and *R. diutinus*, animals were scored as convulsive if they failed to back at least ½ a body length after a touch on the head

with a platinum wire. A more stringent scoring method was employed to compare convulsive phenotypes exhibited by *C. elegans* mutants. Animals were scored as convulsive if animals failed to demonstrate a sinusoidal wave form before or after a touch on the head with a platinum wire and failed to back ½ a body length. Like the convulsion scoring method above, animals treated with acetylcholinesterase inhibitors that failed to demonstrate a sinusoidal wave form before or after a touch on the head with a platinum wire that also fail to back ½ a body length were scored as paralyzed.

Locomotory Radiation Assay

~150 L4/young adult worms were pipetted in a 15 μL droplet onto the centre of a standard 10 cm round culture plate containing MYOB media + agar containing small-molecule with 1% DMSO. Media with drug were prepared in 50 mL falcon tube inverted 10x before pouring. Plates were dried for 90 minutes before being supplemented with a full lawn of OP50 bacteria seeded from a saturated culture of OP50 grown in LB broth. Plates were left uncovered adjacent to a flame until the (~15 minutes). 3 hours after pipetting worms onto plates the plates were flash frozen at -80°C for 3 minutes to freeze worms in place. The fraction of worms that travelled at least 1.65 cm (diameter after measuring 1cm from the edge of the droplet) from centre of the plate were recorded.

Developmental Growth Assay

C. elegans larval development assays were conducted in 96-well flatbottom clear flatbottom plates. ~20 L1 larvae in 10 µL of M9 buffer were pipetted into each test wells containing 40 µL of NGM media supplemented with HB101 *E. coli* with the desired test compound (+0.6% dimethylsulfoxide (DMSO; Sigma-Aldrich product ID: D8418) as the chemical solvent). Plates were wrapped in 3 layers of brown paper towels soaked with water. After either 3 or 6 days of incubation the number of *C. elegans* animals of different larval stages were recorded using a Leica MZ75 stereomicroscope.

C. elegans Confocal Microscopy

C. elegans KG4247 expressing *ceIs201* [unc-17p::ins-22::Venus + unc-17p::RFP + unc-17p::ssmCherry + myo-2p::RFP] were incubated on 6 cm MYOB media + 2% agar plates containing either 60 µM Nementin-1 or 60 µM Nementin-12 with 1% DMSO or 1% DMSO alone for 4 hours at room temperature. Wells were seeded with OP50 *E. coli* bacteria and used the day after preparation (see locomotory survey for further details on the preparation of media + drug plates). After incubation, animals were picked onto a 5% agar pad, 10 µL 10 mM tetramisole hydrochloride (prepared from 99% (–)-tetramisole hydrochloride, Sigma-Aldrich product ID: L9756) solvated in standard M9 buffer was pipetted onto the pad and a cover glass put on top. Animals were imaged using a Leica DMI 6000 B confocal microscope with a Hamatsu C9100-31 camera with a 100x oil immersion objective. A 491 nm laser was used to excite INS-22::Venus and images were captured with 25ms of exposure. A 510 nm laser was used to excite ssmCherry and RFP and images were captured with 100 ms of exposure. Images were

captured after anterior and dorsal nerve cord features were brought into focus in the red channel (the RFP remained stable for the duration of imaging). Anterior, midbody and posterior regions containing respective coelomocytes (ccPR + ccAR, ccPL + ccAL & ccDL respectively) were captured. Images were captured over a 30 µm Z-stack
220 captured with a 0.5 µm step and all images were captured within 25 minutes of slide preparation. A maximal projection containing the ventral and dorsal nerve cords and coelomocyte was generated for each captured section in ImageJ (version 1.52i). Tracings of captured axonal sections and coelomocytes were manually drawn and fluorescence signal measured in ImageJ. Due to the variability in coelomocyte
225 endocytic/lysosomal vesicle content, coelomocytes were reported as the measurement of mean fluorescence signal of the GFP channel compared to the RFP channel. For axonal segments, the mean of two measurements of each region and representative background were collected to adjust for variability in manual measurement. Regions of interest for at least 15 animals were captured over several imaging sessions, at least 3
230 control animals were captured in each imaging session.

Parasitic Nematode Assays

Cooperia oncophora Assay: Fresh cattle feces containing eggs of an ivermectin-resistant strain of *C. oncophora* were kindly supplied by Dr. Doug Colwell and Dawn
235 Gray (Lethbridge Research Station, Agriculture and Agri-Food Canada). Established methods were used to carry out the experimental cattle infections, and these methods were approved by the Lethbridge AAFC Animal Care committee and conducted under

animal use license ACC1407. Cattle faeces containing C*. oncophora* eggs were stored anaerobically at room temperature for a maximum of 6 days before use. Eggs were
240 isolated from faeces using a standard saturated salt flotation method immediately before the egg hatch assay. 80 μl of distilled and deionized water was added to each well of a 96-well culture plate, and then 1 μL of chemical at the appropriate concentration in DMSO was added to each well using a multichannel pipette. Approximately 50 eggs were added per well in 20 μL of water for a final volume of 100
245 μL in each well; the final DMSO concentration was 1% (v/v). The eggs were incubated in the chemicals for 2 days at room temperature, after which hatching was stopped by the addition of 1 μL iodine tincture to each well. The number of hatched larvae was counted at each concentration, and eggs that failed to hatch were scored as dead. "Relative viability" values were calculated by dividing the fraction of eggs that hatched at
250 each concentration by the fraction of eggs that hatched in the corresponding DMSO control well. Two biological replicates were performed for each dose-response experiment, and the relative viability values were averaged across the biological replicates. The average hatch rate for the DMSO control wells was greater than 93% for both biological replicates.

255 *Dirofilaria immitis Assay:* Experiments on *D. immitis* microfilariae were performed in the laboratories of Bayer Animal Health GmbH (Monheim, Germany). The Missouri *D. immitis* isolate used for all assays was originally isolated from an infected dog from Missouri (USA). From 2005 onwards, the isolate was maintained and passaged in beagle dogs at the University of Georgia (Athens, GA, USA). From 2012 onward, the

260 isolate was also maintained at the laboratories of Bayer Animal Health GmbH in Monheim, Germany. For the experiments with microfilariae, blood was sampled from beagle dogs (Marshall BioResources, North Rose, NY, USA) with patent infections, and microfilariae were purified according to the protocol described by the FR3.

Approximately 250 freshly purified microfilariae were cultured in single wells of a 96-
265 well microtiter plate containing supplemented RPMI 1640 medium. Microfilariae exposed to medium substituted with 1% DMSO were used as negative controls. Motility of microfilariae was evaluated after 72 hours of drug exposure using an image-based approach – DiroImager, developed by Bayer Technology Services. This device is a fully automated high-throughput platform, allowing high-resolution optical imaging of an
270 entire 96-well microtiter plate. The DiroImager integrates a high-resolution video camera (Prosilica GT6600; Allied Vision) with a telecentric lens (S5LPJ3005; Sill Optics) that prevents perspective distortion of the recorded images, ensuring high accuracy of measured values across all samples. In brief, a series of 20 high-resolution images were recorded (one per second). In a first step, image processing filters were used that
275 discriminate larger objects to avoid the detection of crystallized or undissolved particles. In the actual calculation, pixel-wise differences between sequential images were calculated to determine worm movement between single images of a series; test compound activity was determined as the reduction of motility in comparison to the solvent control. Based on the evaluation of a wide concentration range, concentration–
280 response curves as well as IC50 values were calculated were applicable.

Nippostrongylus brasiliensis acetylcholine esterase secretion assay: This assay has been previously described in detail (*3*). AChE is secreted by many parasitic nematodes, including *N. brasiliensis*. Assaying a small molecule's impact on AChE secretion is therefore a proxy for its ability to modulate the nematode's nervous system. Methods have been previously developed to assay AChE secretion from *Nippostrongylus* using colourimetric determination of AChE activity in the culture medium (*4*). Briefly, test compounds were dissolved in DMSO at a concentration of X, Y, Z and serial dilutions were performed in DMSO resulting in stock solutions of A, B, C. Stock solutions were stored at -20 °C until they were diluted 1:200 with culture medium (20 g/l Bacto Casitone, 10 g/l yeast extract, 5 g/l glucose, 0.8 g/l KH2PO4, 0.8 g/l K2HPO4, 10 µg/ml sisomycin and 1 µg/ml clotrimazole, pH 7.2). Final drug concentrations were E, F, G *µ*M in 1.0 % DMSO. Because secretion of AChE is gender and body weight specific two female and three male adult worms were placed in each well containing 1 ml of pre-warmed medium with drugs plus vehicle and incubated at 37 °C and 95% relative humidity for five days (*5*). All drug concentrations were performed in duplicate. From each well 25 µl medium were transferred into a 96 well plate. Then, 250 µl 5,5′-dithio-bis (2-nitrobenzoic acid) (0.25 µM) and 25 µl acetylthiocholine (4 mM) were added. AChE cleaves acetylthiocholine into acetate and thiocholine. In a consecutive reaction, thiocholine reacts with 5,5′-dithio-bis(2- nitrobenzoic acid) to thionitrobenzoate. Thionitrobenzoate is a yellow dye and its concentration can be determined by measuring the absorption at 405 nm. The A405 was measured after two and seven minutes of incubation at RT using an Expert 96 plate reader (Asys-Hitech, Salzburg,

Austria) and the software MikroWin 2000 (Mikrotek, Overrath, Germany). The difference in absorption between both time points was taken as measure of AChE activity. The
305 arithmetic mean of 12 no drug control wells was set to 100% activity, and reduction of AChE activity in percentage relative to the negative control was calculated for each test compound concentrations. Within an assay, every drug concentration was performed in duplicate, and the software reported the mean of these duplicates.

Strongyloides ratti L3 larvae lethality: Data are the measurement of the % of Larval
310 stage 3 (L3) worms (as indicated) that respond to 80°C hot water stimulus after 24 hours or 72 hours of incubation in wells containing the indicated compound. Data are the mean measurement of 30-40 larvae incubated in a dark box at room temperature for 24 or 72h over duplicate biological replicate conducted in triplicate.

Trichuris muris L1 larvae experiments: T. muris eggs were collected from the feces
315 of the infected mice (as described above) using a flotation method with saturated NaCl solution in Milli-Q water. *T. muris* eggs were stored in Milli-Q water in the dark for 3 months at 23-25°C, until the eggs were embryonated. *T. muris* L1 were obtained using a hatching procedure with *E. coli(6)*. 30-40 larvae were placed in each well of a 96-well plate containing 175 *µ*l culture medium and 25 *µ*l of the test drug stock solutions. Larvae
320 were kept at 37°C, 5% CO_2 for 24 hours. To evaluate the drug effect first the total number of L1 per well was determined. Then, 50-80 *µ*l of hot water (≈80°C) was added to each well and the larvae that responded to this stimulus were counted. The proportion of larval death was determined. Larval survival counts were averaged over duplicate biological replicate conducted in triplicate normalized to controls.

325 *T. muris adult experiments:* Mice (C57BL/6NRj) were infected with 200 embryonated *T. muris* eggs. Seven weeks post-infection *T. muris* adult worms were collected from the intestines. Three worms were placed in each well of a 24-well plate containing 1980 μl culture medium and 20 μl of the test drugs (10 μM of a 1mM stock solution). After 72 hours of incubation at 37°C, 5% CO_2 the condition of the worms was microscopically
330 evaluated using a viability scale from 3 (normal activity) to 0 (dead). Viability scores were averaged across replicates and normalized to the control wells. The experiment was conducted in duplicate.

Heligmosomoides polygyrus L3 viability: H. polygyrus infection three-week-old female NMRI mice were obtained from Charles River (Sulzfeld, Germany). Rodents
335 were kept under environmentally-controlled conditions (temperature: 25°C, humidity: 70%, light/dark cycle 12 h /12 h) and had free access to water (municipal tap water supply) and rodent food and were allowed to acclimatize for one week. NMRI mice were infected with 88 *H. polygyrus* L3. Two weeks post-infection, mice were dissected cultivating the eggs on an agar plate for 8-10 days in the dark at 24°C. For the assays,
340 30-40 larvae were placed in each well of a 96-well plate containing 175 μl culture medium and 25 μl of the test drug stock solutions. *H. polygyrus* adults and stage 3 larvae (L3) were incubated in RPMI 1640 (Gibco, Waltham MA, USA) medium supplemented with 5% amphotericin B (250 μg/ml, Sigma-Aldrich, Buchs, Switzerland) and 1% penicillin 10,000 U/ml, and streptomycin 10 mg/ml solution (Sigma-Aldrich,
345 Buchs, Switzerland). Culture plates were kept in a dark box at room temperature for up to 72 hours. To evaluate the drug effect first the total number of L3 per well was

determined. Then, 50-80 μl of hot water (≈80°C) was added to each well and the larvae that responded to this stimulus were counted. The proportion of larval death was determined. Larval survival counts were averaged over duplicate biological replicate
350 conducted in triplicate normalized to controls.

Necator americanus L3 viability: N. americanus larvae (L3) were obtained by filtering the feces of infected hamsters and cultivating the eggs on an agar plate for 8-10 days in the dark at 24°C. *Necator americanus* L3 were incubated in Hanks' balanced salt solution (HBSS; Gibco, Waltham MA, USA) supplemented with 10% amphotericin B and
355 1% penicillin (10,000 U/ml) and streptomycin (10 mg/ml) solution. For the assays, 30-40 larvae were placed in each well of a 96-well plate containing 175 μl culture medium and 25 μl of the test drug stock solutions. Treated Larvae were kept in a dark box at room temperature for up to 72 hours. To evaluate the drug effect first the total number L3 per well was determined. Then, 50-80 μl of hot water (≈80°C) was added to each well and
360 the larvae that responded to this stimulus were counted. The proportion of larval death was determined. Larval survival counts were averaged over duplicate biological replicate conducted in triplicate normalized to controls.

Meloidogyne incognita assays: M. incognita infective second stage juvenile (J2) in vitro viability assays were performed in 96-well polystyrene plates. Each well contained
365 approximately 25 J2s and compounds were added at a final concentration of 45 μM (0.5% DMSO v/v) in a total volume of 100 μL of sterile distilled water. Plates were sealed with parafilm and incubated for 72 hours at 25 °C. At the end point the fraction of viable nematodes in each drug condition and DMSO solvent controls was calculated by

dividing the number of mobile nematodes by the total number of nematodes in the well.
370 The experiment was conducted twice, with three technical replicates per treatment in each trial. *M. incognita* egg hatching assays were performed in sterile distilled water in 96-well plates similarly to the J2 viability assays described. Embryos were incubated in 45 μM (0.5% DMSO v/v) compound for 7 days at 25 °C. At the end point the number of hatched embryos was quantified in each condition and DMSO solvent controls. The
375 fraction of hatched juveniles that were mobile was also quantified ('hatchling mobility'). The experiment was conducted twice, once with 50 embryos plated per well and once with 100 embryos plated per well, with three technical replicates per treatment in each trial. *M. incognita* 50-day soil reproduction assays were conducted in 90 grams of soil (1:1 sand:loam mix) per compartment in 6-pack planting containers. The soil was
380 drenched with 18 mL of deionized water containing dissolved chemical or DMSO solvent alone. Approximately 1500 J2s were inoculated into the soil in 2 mL of water, for a total volume of 20 mL. The J2s were incubated in the soil and chemical for 24 hours after which a 2-3 week old tomato seedling was transplanted into the soil. Tomatoes were grown for 8 weeks in a greenhouse under long-day conditions (16 hour
385 photoperiod) with 26/18 °C day/night temperatures. At the end point of the assay the tomato roots were harvested and eggs were extracted by rinsing in 0.6% sodium hypochlorite solution with agitation at 300 rpm for 3 minutes. Roots were rinsed with water over nested sieves and eggs present in each root system were collected and quantified. Roots were dried in a 65 °C oven and the number of eggs per milligram of

390 dried root material was calculated. The experiment was conducted twice, with two technical replicates per treatment in each trial.

Meloidogyne hapla motor assay: M. hapla motor assays were conducted using J2 infective larvae isolated from ornamental tomato plant roots. J2s were isolated by isolating egg masses from the root network of infected plants and hatching in deionized
395 water at room temperature for ~1 week. 10 µL of deionized water containing ~15 J2s (no fewer than 10 J2s) were pipetted into 96-well polystyrene plates containing the drug condition of interest with 0.6% DMSO. Addition of J2s to wells were staggered by 35 seconds for the purpose of maintaining a stringent endpoint. Drug dilutions were prepared from stock plates using a 96-well pinner tool (FP3S200 V&P Scientific, Inc.)
400 transferring 0.3 mL of drug stock solution prepared in DMSO. Animals were incubated at room temperature with shaking for 4 hours (100 RPM; helps concentrate J2s in the middle of wells). At the 4 hour endpoint, 30 second videos of each well were captured using a Leica FLEXACAM C1 USB camera mounted to a Leica MZ75 stereomicroscope using Leica LAS EZ image capture software (V3.4.0). Videos were sped up 5x and the
405 number of head turns was used as a read-out of J2 motility. Motility relative to control over three or four biological replicates was calculated & used as the data read-out for the SynergyFinder 2.0 server (https://synergyfinder.fimm.fi/).

Small-Molecule Tanimoto Coefficient Pairwise Similarity

410 Pairwise similarity scores were calculated as the Tanimoto coefficient of shared FP2 fingerprints using OpenBabel (http://openbabel.org). A Further description of Tanimoto

pairwise similarity is provided in Burns et al. 2015 *(26)*. Network visualization for Fig. 1b was performed using Cytoscape (version 3.7.2).

415 Zebrafish Chemical Treatments and Phenotypic Analyses

All phenotypic analysis was performed on a stereomicroscope. At 1 dpf, 5 embryos were placed in 1 mL filter-sterilized egg water with chemicals in sterile 24-well plates (Falcon). At 3dpf, larvae were anaesthetized with ~0.6 mM tricaine methanesulfonate (tricaine), mounted in 3% methylcellulose on glass slides and bright-field images were
420 taken with a 4x objective using a light microscope (Olympus BX43). The morphology of embryos relative to vehicle controls was assessed including their size, presence of edema, heart rate (normal, slow, or nearly absent), and presence of necrosis.

All chemicals were prepared in DMSO and added to filter-sterilized egg water at 0.1% of the final volume. Equal volumes of vehicle solvent were used in all conditions for a
425 single assay. Note that methylene blue was not added to the egg water in any chemical assays. Culture plates were sealed with parafilm, wrapped in aluminum foil, and incubated at 28.5°C until the assay date.

A photoactivation assay was used to elicit movement and assess locomotion of zebrafish larvae as previously described (*7*). At 1 dpf, embryos in their chorions were
430 aliquoted into 150 µL system water in 96-well plates (Falcon). Next, 50 µL of 4X chemical was added to each well to bring the volume to 200µL and 1X final concentration (either 3.75-60 µM). Plates were incubated until 3dpf, at which time any

embryos still in their chorions were manually dechorionated in their wells. To assay locomotion, 10 µL of 210 µM optovin analog 6b8 (ChemDiv ID#2149-0111 or ChemBridge ID#5707191) was added to each well for a final concentration of 10 µM, incubated for 5 min, and movement tracked on the ZebraBox platform (ViewPoint) using a 30s lights on/off for 3m30s.

Arabidopsis thaliana Greening Assay

Greening experiments were performed with *Arabidopsis thaliana* seeds of wild type Col-0; seeds were surface sterilized in bleach and plated onto 0.5X MS, 0.5% sucrose agar medium supplemented with compounds of interest at 5, 15 and 45μM concentrations (0.2% DMSO (v/v/)). After 4d of stratification at 4°C, plates were transferred to a growth chamber (16h / 8h, 150 μE/m^2) and greening recorded after 4 days. Pictures were recorded by camera (SONY a7s) with FE1.8/55 lens (FE 55 mm F1.8 ZA; SEL55F18Z). Experiments were performed in triplicate for each treatment.

Drosophila melanogaster Dose-Response Assay

Fly food in agar substrate was prepared by mixing 100 mL of unsulfured molasses, 100 mL of cornmeal, 41.2 g of Baker's yeast, and 14.8 g of agar into 1400 mL of distilled de-ionized water and boiling for 30 minutes. The media was allowed to cool to 56°C, at which point 5 mL was added by syringe to plastic cylindrical fly vials. 10 μL of chemical, or DMSO alone, was added to the media in each vial. The chemicals were mixed into

the media by mechanical mixing using a pipette. The final DMSO concentration was 0.2% (v/v). The media was allowed to solidify at room temperature (~22°C) overnight. The following day (Day 0), eight pairs of male and female w1118 flies were added to each vial so that there were 16 flies in total per vial. The vials were stored at room temperature for 7 days, at which point the number of mobile flies was counted. Fly mobility was scored as any observable movement after the vial had been vigorously jostled. “Relative mobility” was calculated by dividing the number of mobile flies in the treatment vials by the average number of mobile flies in two DMSO control vials. On Day 8 the 16 parental flies were removed from the vials and the progeny larvae were allowed to continue to grow and hatch into adult flies. To assess larval viability, hatched flies were counted and discarded on Days 10, 12, 14, 16, 18, and 20. The counts were summed. “Relative viability” was calculated by dividing the number of hatched flies in the treatment vials by the average number of hatched flies in the two DMSO control vials. The final “relative mobility” and “relative viability” values are an average across three experimental replicates.

HEK293 Proliferation Assay

HEK293 cells were seeded into 96 well plates, at 5000 cells per well, in 100 μL total volumes of DMEM/10%FBS/1%PS media and grown overnight at 37˚C in the presence of 5% CO_2. Compounds (0.5 μL volumes from appropriate source plates) were then added to cells, and growth was continued for an additional 48 hours. Following growth, 10 μL of CellTiter-Blue Viability reagent (Promega) was added to each well, and plates

were incubated for an additional 4 hours at 37˚C in the presence of 5% CO_2. Fluorescence measurements (560 nm excitation/590 nm emission) were then performed using a CLARIOstar Plate Reader (BMG Labtech) to quantify reagent reduction and estimate cell viability.

480

Spicule Protraction Assay

L4 males grown overnight on Nematode Growth Media (NGM) 2% agar plates + OP50. Next day adult males plated in liquid NGM liquid culture with 1% DMSO or 60 µM Nementin-1 with 1% DMSO in polystyrene 96-well plates. Adults were observed under a
485 Leica MZ75 stereomicroscope at indicated time points. Reported '% Protracted' includes partial spicule protraction.

Statistical Analyses & Synergy Modelling

Unpaired one or two-sided t-tests or one-sided ANOVA with Dunnett's adjustment for
490 multiple comparisons were conducted between control and treatment groups with where appropriate. Two-sided Chi-square tests with Bonferroni correction were conducted for comparison of proportional convulsion data to respective controls. Extra sum-of-squares F tests were conducted comparing EC50 curves generated for dose-response data. Statistical analyses were conducted using GraphPad Prism (version 9). Zero-Interaction
495 Potency (ZIP) synergy scores and heatmaps were generated using the SynergyFinder2.0 server using the default parameter set.

Chemistry

General Considerations:

Unless otherwise stated, all reactions were set up under inert atmosphere (argon) utilizing glassware (or 2 dram vials) that were flame-dried and cooled under argon purging. Unless otherwise stated, flash column chromatography was performed on Silicycle® Siliaflash® P60, 40-63 µm silica gel. Starting materials and catalysts were purchased from commercial suppliers (Sigma Aldrich, Strem, Alfa Aesar, TCI or Combi-Blocks) and used without further purification unless otherwise stated. All solvents were distilled, purified, and dried according to standard procedures. Reactions were monitored using thin-layer chromatography (TLC) on EMD Silica Gel 60 F254 plates. Visualization of the developed plates was performed under UV light (254 nm) or by immersion in Ceric Ammonium Molybdate (CAM) or Potassium Permanganate ($KMnO_4$) stains.

NMR characterization data was collected at 296 K on a Varian Mercury 300, Varian Mercury 400, Bruker Avance III 400, Agilent DD2 500 (with cold probe), or an Agilent DD2 600 operating at 300, 400, 500, or 600 MHz for ^{1}H NMR, and 75, 100, 125, or 150 MHz for ^{13}C NMR. (Funded by the Canadian Foundation for Innovation, project number 19119, and the Ontario MRI). ^{1}H NMR spectra were internally referenced to the solvent residual signal ($CDCl_3$ = 7.26 ppm) unless otherwise stated. ^{13}C NMR spectra were internally referenced to the residual solvent signal (CDCl3 = 77.16 ppm) unless otherwise stated. ^{19}F NMR spectra were externally referenced to $CFCl_3$. Data for ^{1}H NMR are reported as follows: chemical shift (δ ppm), multiplicity (s = singlet, d =

doublet, t = triplet, q = quartet, m = multiplet, br = broad), coupling constant (Hz),
520 integration.

Melting point (mp) ranges were determined on a Fisher-Johns® Melting Point Apparatus and are reported uncorrected.

Infrared (IR) spectra were acquired using a Shimadzu FTIR-8400S FT-IR spectrometer as thin films ($CHCl_3$ or CH_2Cl_2) or neat on NaCl plates. Data is presented
525 in wavenumbers (ν_{max}, cm^{-1}).

High Resolution Mass Spectra (HRMS) were obtained on a micromass 70S-250 spectrometer (EI) or an AB SCIEX QSTAR® Mass Spectrometer (ESI) or a JEOL® AccuTOF medel JMS-T1000LC mass spectrometer equipped with an IONICS® Direct Analysis in real Time (DART) ion source at Advanced Instrumentation For Molecular
530 Structure (AIMS) in the Department of Chemistry at the University of Toronto. Where ESI+ was employed, the values correspond to the *ionic species of interest* and the given ionic formula includes the charging agent (H^+ or Na^+); both the measured and calculated values *are corrected* for the mass of the electron and are reported as *m/z*. The DART-MS accurate mass report is generated using the
535 *Elemental Composition Estimation* feature as implemented in the JEOL *Mass Centre* software package. Where DART was employed, the measured values correspond to the *neutral species of interest* and the given molecular formula includes the charging agent (H^+ or NH_4^+); the measured and calculated values *are not corrected* for the mass of the electron and are reported as *neutral masses*.

540

General Procedures for the Synthesis

General Procedure A – Wittig Reaction

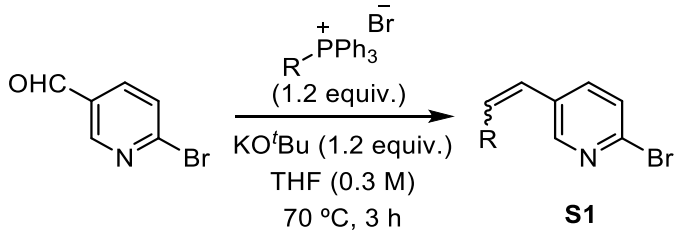

The phosphonium salt (1.2 equiv.) was first dissolved in THF (0.3 M). KO^{t}Bu (1.2 equiv.) was then added and the mixture was stirred at room temperature for 30 minutes. The pyridinecarboxaldehyde (1 equiv.) was then added in three portions and the reaction was refluxed at 70 °C for 3 hours. The mixture was then allowed to cool to room temperature and was filtered through a Celite pad eluting with pentanes. The filtrate was concentrated *in vacuo* and the product (mixture of isomers) was purified by flash column chromatography, eluting with a mixture of EtOAc:pentanes.

General Procedure B – Suzuki Reaction (8)

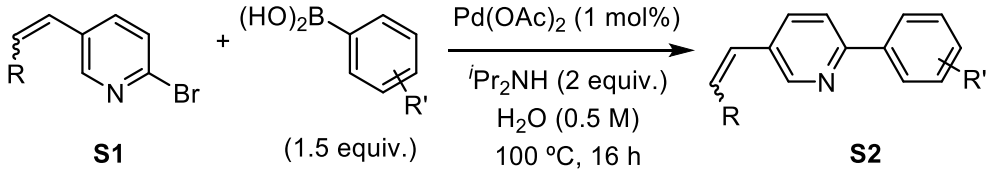

Substituted aryl boronic acid (1.5 equiv.) and $Pd(OAc)_2$ (1 mol%) were added to a mixture of the substituted bromopyridine (1 equiv.) in water (0.5 M). ^{i}Pr$_2$NH (2 equiv.) was then added and the reaction was refluxed at 100 °C for 16 hours. The mixture was allowed to cool to room temperature and brine was added. The aqueous phase was

extracted with ethyl acetate. The combined organics was washed with brine, dried with $MgSO_4$, and concentrated *in vacuo*. The product was purified by flash column chromatography, eluting with a mixture of EtOAc:pentanes.

General Procedure C – Hydrogenation

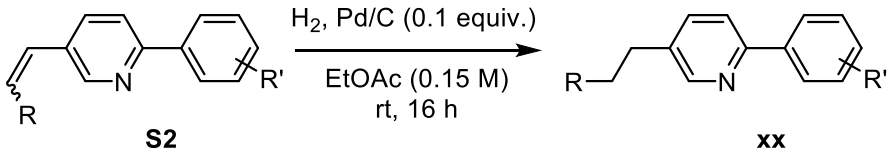

The vinylbiarene was dissolved in EtOAc (0.15 M). Pd/C (3% Pd, total 10 mol% Pd used) was added. Three cycles of evacuation and backfill with argon, followed by H_2 from a balloon was carried out. The reaction was stirred at room temperature under a H_2 atmosphere (balloon) for 16 hours. The contents of the flask were filtered over a Celite pad eluting with EtOAc and concentrated *in vacuo*. The product was purified by flash column chromatography, eluting with a mixture of EtOAc:pentanes.

2-(4-((difluoromethyl)thio)phenyl)-5-propylpyridine [nementin-12-5(C), YHK01-077F1]

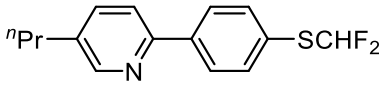

xx was synthesized according to General Procedure A, B, and C using 6-bromonicotinaldehyde, ethyltriphenylphosphonium bromide, and (4-((difluoromethyl)thio)phenyl)boronic acid with an overall yield of 21%.

4-(difluoromethoxy)-4'-propyl-1,1'-biphenyl [nementin-12-6(D), KLC10-089F1]

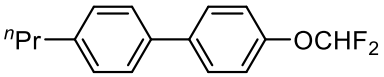

xx was synthesized according to General Procedure A, B, and C using 4-bromobenzaldehyde, ethyltriphenylphosphonium bromide, and (4-(difluoromethoxy)phenyl)boronic acid with an overall yield of xx%.

5-(4-(difluoromethoxy)phenyl)-2-propylpyridine [nementin-12-7, YHK01-104F1]

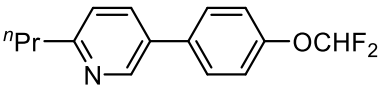

xx was synthesized according to General Procedure A, B, and C using 5-bromopicolinaldehyde, ethyltriphenylphosphonium bromide, and (4-(difluoromethoxy)phenyl)boronic acid with an overall yield of 16%.

5-(difluoromethoxy)-2-(4-propylphenyl)pyridine [nementin-12-8, YHK01-102F1]

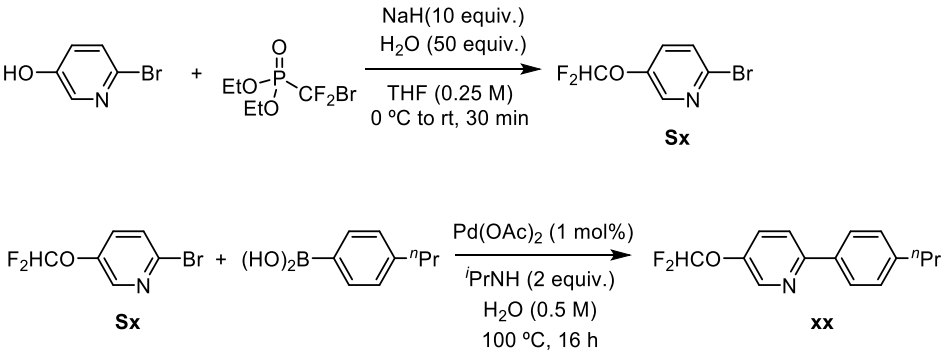

2-bromo-5-(difluoromethoxy)pyridine (Sx): The procedure was adapted from Geng et al. *(9).* 6-bromopyridin-3-ol (348 mg, 2 mmol, 1 equiv.) was dissolved in THF (8 mL, 0.25 M) and cooled to 0 °C. NaH (800 mg, 20 mmol, 60%, 10 equiv.) was added and

the mixture was stirred at 0 °C for 30 minutes. H_2O (1.80 mL, 100 mmol, 50 equiv.) was added dropwise and the mixture was stirred at 0 °C for 10 minutes. Diethyl (bromodifluoromethyl)phosphonate (0.71 mL, 4 mmol, 2 equiv.) was added and the reaction was allowed to stir from 0 °C to room temperature for 30 minutes. H_2O was added and the aqueous phase was extracted with EtOAc. The combined organics was washed with brine, dried with $MgSO_4$, and concentrated *in vacuo*. The crude mixture was purified by flash column chromatography, eluting with 5% (v/v) EtOAc:pentanes to give **xx** (161.1 mg, 0.72 mmol, 36%).

5-(difluoromethoxy)-2-(4-propylphenyl)pyridine (xx): Suzuki reaction was carried out to couple **Sx** (161.1 mg, 0.72 mmol, 1 equiv.) and (4-propylphenyl)boronic acid (177.1 mg, 1.08 mmol, 1.5 equiv.) according to General Procedure B to give **Sx** (140.0 mg, 0.53 mmol, 74%).

2-(difluoromethoxy)-5-(4-propylphenyl)pyridine [nementin-12-9, YHK01-095F1]

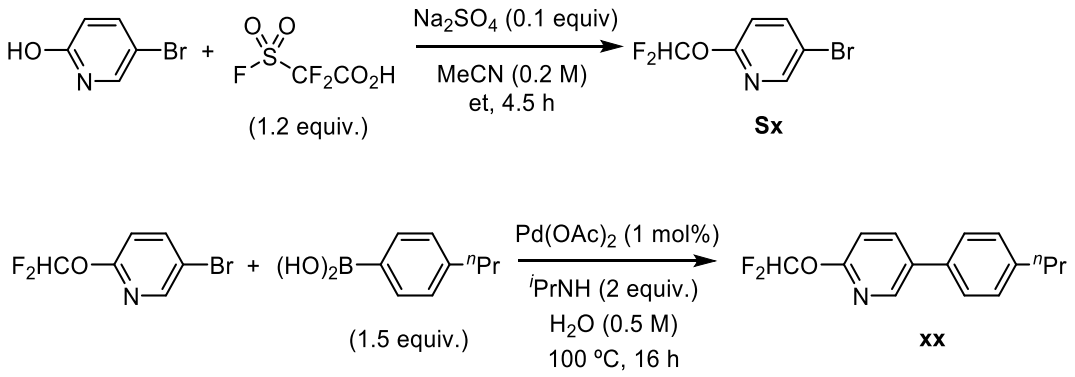

5-bromo-2-(difluoromethoxy)pyridine (Sx): The procedure was adapted from Ando *et al. (10).* 5-bromopyridin-2-ol (870 mg, 5 mmol, 1 equiv.) was dissolved in MeCN (25 mL, 0.2 M). 2,2-difluoro-2-(fluorosulfonyl)acetic acid (0.67 mL, 6 mmol, 1.2 equiv.) was added, followed by Na_2SO_4 (7.1 mg, 0.5 mmol, 0.1 equiv.). The reaction was quenched with saturated $NaHCO_{3(aq)}$ solution and extracted with EtOAC. The combined organics was washed with brine, dried with $MgSO_4$, and concentrated *in vacuo*. The crude mixture was purified by flash column chromatography, eluting with a 5 to 10% (v/v) EtOAc:pentanes gradient to give **Sx** (521.9 mg, 2.3 mmol, 47%).

2-(difluoromethoxy)-5-(4-propylphenyl)pyridine (xx): Suzuki reaction was carried out to couple **Sx** (112.0 mg, 0.5 mmol, 1 equiv.) and (4-propylphenyl)boronic acid (123.0 mg, 0.75 mmol, 1.5 equiv.) according to General Procedure B to give **xx** (114.0 mg, 0.433 mmol, 87%).

2-(4-(difluoromethoxy)phenyl)-5-ethylpyridine [nementin-12-10(E), YHK01-040F1]

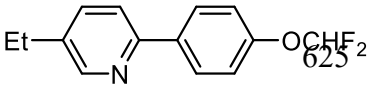

xx was synthesized according to General Procedure A, B, and C using 6-bromonicotinaldehyde, methyltriphenylphosphonium bromide, and (4-(difluoromethoxy)phenyl)boronic acid with an overall yield of 4%.

2-(4-(difluoromethoxy)phenyl)-5-methylpyridine [nementin-12-11, YHK01-122Rec]

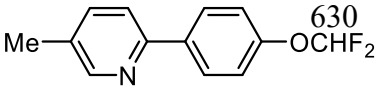

xx was synthesized according to General Procedure B using 2-bromo-5-methylpyridine and (4-(difluoromethoxy)phenyl)boronic acid with a yield of 14%.

2-(4-(difluoromethoxy)phenyl)pyridine [nementin-12-12, YHK01-007C2F1]

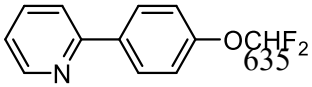

xx was synthesized according to General Procedure B using 2-bromopyridine and (4-(difluoromethoxy)phenyl)boronic acid with a yield of 31%.

2-(4-(difluoromethoxy)phenyl)-5-(prop-1-yn-1-yl)pyridine [nementin-12-14, YHK01-082, 085, 091, 094F1]

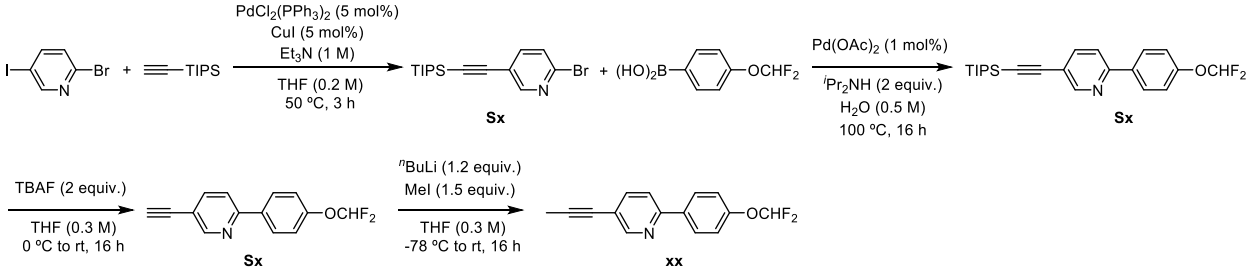

2-bromo-5-((triisopropylsilyl)ethynyl)pyridine (Sx): 2-bromo-5-iodopyridine (283.4 mg, 1 mmol, 1 equiv.), $PdCl_2(PPh_3)_2$ (35.1 mg, 0.05 mmol, 5 mol%), and CuI (9.5 mg, 0.05 mmol, 5 mol%) were weighed into a flame-dried round bottom flask. The contents were purged under nitrogen for 5 minutes. THF (6 mL, 0.2 M) was then added to the flask. Et_3N (1 mL, 1 M) and ethynyltriisopropylsilane (0.27 mL, 1.2 mmol, 1.2 equiv.) were added subsequently. The reaction was stirred at 50 °C for 3 hours. The mixture

was cooled to room temperature and then filtered through celite, eluting with EtOAc. The filtrate was concentrated *in vacuo* and the crude mixture was purified by flash column chromatography, eluting with 10% (v/v) EtOAc:pentanes to give **Sx** (235.6 mg, 0.70 mmol, 70%)

2-(4-(difluoromethoxy)phenyl)-5-((triisopropylsilyl)ethynyl)pyridine (Sx): Suzuki reaction was carried out to couple **Sx** (235.6 mg, 0.70 mmol, 1 equiv.) and (4-(difluoromethoxy)phenyl)boronic acid (0.197 mg, 1.05 mmol, 1.5 equiv.) according to General Procedure B to give **Sx** (161.9 mg, 0.40 mmol, 58%).

2-(4-(difluoromethoxy)phenyl)-5-ethynylpyridine (Sx): **Sx** (162.0 mg, 0.4 mmol, 1 equiv.) was dissolved in THF (1.3 mL, 0.3 M) and cooled to 0 °C. TBAF (0.8 mL, 0.8 mmol, 1 M in THF, 2 equiv.) was added dropwise. The reaction was allowed to stir from 0 °C to room temperature for 16 hours. H_2O was added and the aqueous phase was extracted with EtOAc. The combined organics was washed with brine, dried with $MgSO_4$, and concentrated *in vacuo*. The crude mixture was purified by flash column chromatography, eluting with a 5 to 10% (v/v) EtOAc:pentanes gradient to give **Sx** (76.5 mg, 0.31 mmol, 78%).

2-(4-(difluoromethoxy)phenyl)-5-(prop-1-yn-1-yl)pyridine (xx): **Sx** (77.0 mg, 0.31 mmol, 1 equiv.) was dissolved in THF (1.0 mL, 0.3 M) and cooled to -78 °C. ^{n}BuLi (0.15

mL, 0.37 mmol, 2.5 M in hexane, 1.2 equiv.) was added dropwise. The mixture was stirred at -78 °C for 1 hour. Iodomethane (0.03 mL, 0.47 mmol, 1.5 equiv.) was added dropwise. The reaction was allowed to stir from -78 °C to room temperature for 16 hours. The reaction was quenched with saturated $NH_4Cl_{(aq)}$ solution and extracted with EtOAc. The combined organics was washed with brine, dried with $MgSO_4$, and concentrated *in vacuo*. The crude mixture was purified by flash column chromatography, eluting with a 2.5 to 5% (v/v) EtOAc:pentanes gradient to give **xx** (28.3 mg, 0.11 mmol, 35%).

(6-(4-(difluoromethoxy)phenyl)pyridin-3-yl)methanamine [nementin-12-17, YHK01-061, 098, 108, 112, 119, 120, 123Cr]

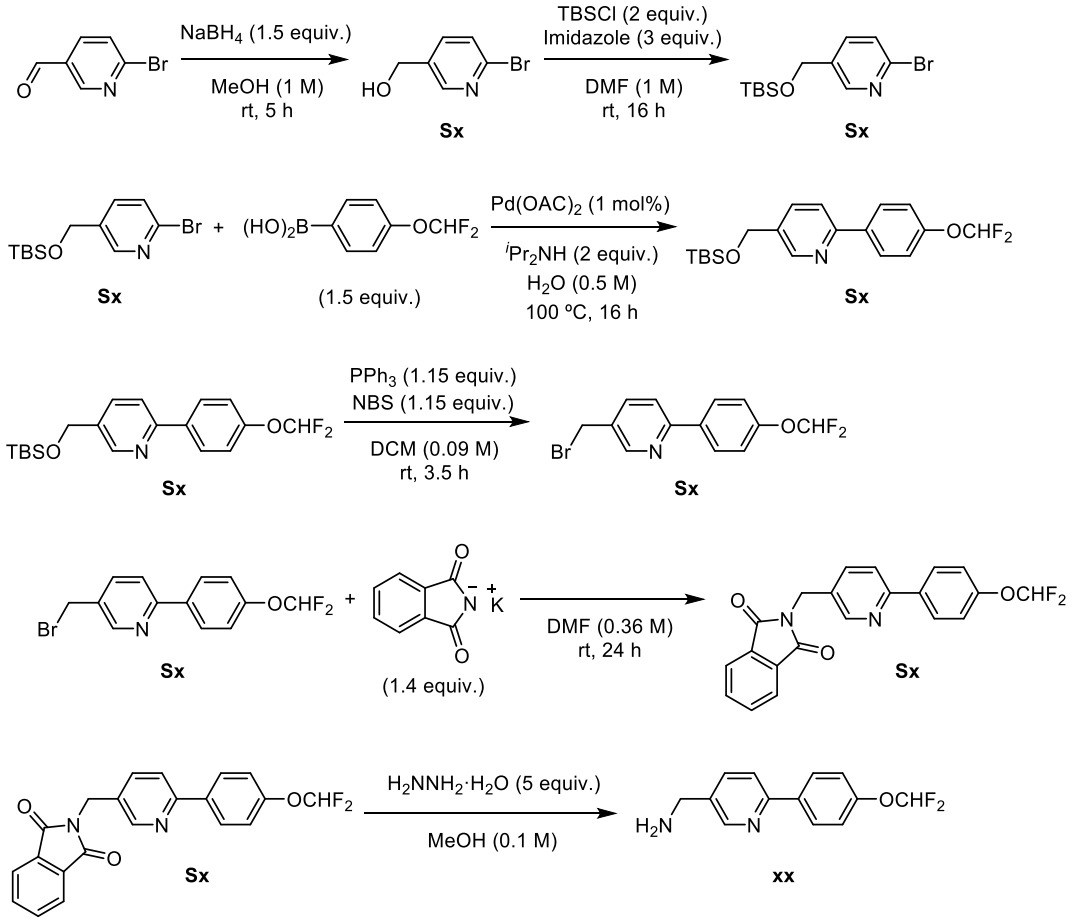

(6-bromopyridin-3-yl)methanol (Sx): 6-bromonicotinaldehyde (1.302 g, 7 mmol, 1 equiv.) was dissolved in MeOH (7 mL, 1 M). $NaBH_4$ (397.0 mg, 10.5 mmol, 1.5 equiv.) was added in three portions. The reaction was stirred at room temperature for 5 hours. The mixture was then cooled to 0 °C and 1 M HCl was added dropwise until bubbling seized, followed with dilution of the mixture with H_2O. The aqueous phase was extracted with EtOAc. The combined organics was washed with brine, dried with

$MgSO_4$, and concentrated *in vacuo*. The crude mixture was purified by flash column chromatography, eluting with a 50 to 60% (v/v) EtOAc:pentanes gradient to give **Sx** (1.2859 g, 6.84 mmol, 98%).

2-bromo-5-(((tert-butyldimethylsilyl)oxy)methyl)pyridine (Sx): **Sx** (884.0 mg, 4.7 mmol, 1 equiv.) was dissolved in DMF (4.7 mL, 1 M) and cooled to 0 °C. TBSCl (1.4160 g, 9.4 mmol, 2 equiv.) was added followed by imidazole (960.0 mg, 14.1 mmol, 3 equiv.). The reaction was allowed to stir from 0 °C to room temperature for 16 hours. H_2O was added to the mixture and the aqueous phase was extracted with EtOAc. The combined organics was washed with brine, dried with $MgSO_4$, and concentrated *in vacuo*. The crude mixture was purified by flash column chromatography, eluting with a 1 to 2% (v/v) EtOAc:pentanes gradient to give **xx** (1.0952 g, 3.63 mmol, 77%).

5-(((tert-butyldimethylsilyl)oxy)methyl)-2-(4-(difluoromethoxy)phenyl)pyridine (Sx): Suzuki reaction was carried out to couple **Sx** (1.0900 g, 3.63 mmol, 1 equiv.) and (4-(difluoromethoxy)phenyl)boronic acid (1.0200 g, 5.45 mmol, 1.5 equiv.) according to General Procedure B to give **Sx** (751.6 mg, 1.98 mmol, 54%).

(6-(4-(difluoromethoxy)phenyl)pyridin-3-yl)methanol (Sx): **Sx** (751.6 mg, 1.98 mmol, 1 equiv.) was dissolved in THF (6.6 mL, 0.3 M) and cooled to 0 °C. TBAF (2.38 mL, 2.38 mmol, 1 M in THF, 1.2 equiv.) was added dropwise. The reaction was allowed to

710 stir from 0 °C to room temperature for 16 hours. H_2O was added to the mixture and the aqueous phase was extracted with EtOAc. The combined organics was washed with brine, dried with $MgSO_4$, and concentrated *in vacuo*. The crude mixture was purified by flash column chromatography, eluting with a 50 to 60% (v/v) EtOAc:pentanes gradient to give **Sx** (363.0 mg, 1.45 mmol, 73%).

715

5-(bromomethyl)-2-(4-(difluoromethoxy)phenyl)pyridine (Sx): **Sx** (363.0 mg, 1.45 mmol, 1 equiv.) was dissolved in DCM (16.11 mL, 0.09 M). PPh_3 (438.0 mg, 1.67 mmol, 1.15 equiv.) followed by NBS (297.2 mg, 1.67 mmol, 1.15 equiv.) were added. The reaction was stirred at room temperature for 3.5 hours. H_2O was added to the mixture

720 and the aqueous phase was extracted with EtOAc. The combined organics was washed with brine, dried with $MgSO_4$, and concentrated *in vacuo*. The crude mixture was purified by flash column chromatography, eluting with a 15% (v/v) EtOAc:pentanes to give **Sx** (349.5 mg, 1.11 mmol, 77%).

725 **2-((6-(4-(difluoromethoxy)phenyl)pyridin-3-yl)methyl)isoindoline-1,3-dione (Sx)**: **Sx** (349.5 mg, 1.11 mmol, 1 equiv.) was dissolved in DMF (3.1 mL, 0.36 M). Phthalimide potassium salt (438.0 mg, 1.67 mmol, 1.15 equiv.) was added. The reaction was stirred at room temperature for 24 hours. H_2O was added to the mixture and the aqueous phase was extracted with EtOAc. The combined organics was washed with brine, dried

730 with $MgSO_4$, and concentrated *in vacuo*. The crude mixture was purified by flash

column chromatography, eluting with a 20 to 25% (v/v) EtOAc:pentanes gradient to give **Sx** (262.2 mg, 0.69 mmol, 62%).

(6-(4-(difluoromethoxy)phenyl)pyridin-3-yl)methanamine (xx): **Sx** (262.2 mg, 0.69 mmol, 1 equiv.) was dissolved in MeOH (6.9 mL, 0.1 M). Hydrazine hydrate (0.26 mL, 3.56 mmol, 50-60%, 5 equiv.) was added. The reaction was refluxed at 70 °C for 4 hours. The mixture was cooled to room temperature and filtered through Celite, eluting with MeOH. The filtrate was concentrated *in vacuo*. H_2O (7 mL) was added, followed by 1 M KOH (1.75 mL). The aqueous phase was extracted with DCM. The combined organics was dried with $MgSO_4$ and then concentrated *in vacuo* to give **xx** (131.4 mg, 0.53 mmol, 76%).

2-(4-(difluoromethoxy)phenyl)-6-propylpyridine [nementin-12-20(F), YHK01-034C2F1]

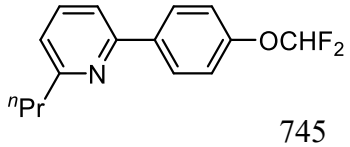

xx was synthesized according to General Procedure A, B, and C using 6-bromopicolinaldehyde, ethyltriphenylphosphonium bromide, and (4-(difluoromethoxy)phenyl)boronic acid with an overall yield of 18%.

2-(4-(difluoromethoxy)phenyl)-4-propylpyridine [nementin-12-21(G), YHK01-152F1]

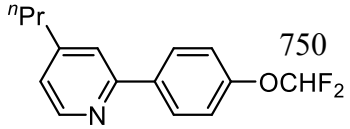

xx was synthesized according to General Procedure A, B, and C using 2-bromoisonicotinaldehyde, ethyltriphenylphosphonium bromide, and (4-(difluoromethoxy)phenyl)boronic acid with an overall yield of 9%.

2-(4-(difluoromethoxy)phenyl)-3-propylpyridine [nementin-12-22(H), YHK01-014F1]

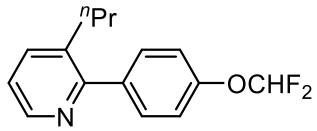

xx was synthesized according to General Procedure A, B, and C using 2-bromonicotinaldehyde, ethyltriphenylphosphonium bromide, and (4-(difluoromethoxy)phenyl)boronic acid with an overall yield of 6%.

2-(3-(difluoromethoxy)phenyl)-5-propylpyridine [nementin-12-23(I), YHK01-036F1]

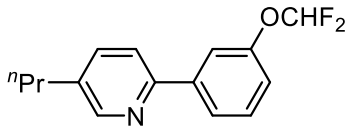

xx was synthesized according to General Procedure A, B, and C using 6-bromonicotinaldehyde, ethyltriphenylphosphonium bromide, and (3-(difluoromethoxy)phenyl)boronic acid with an overall yield of 21%.

2-(4-(difluoromethoxy)phenyl)-5-propylpyrimidine [nementin-12-25, KLC11-041F1]

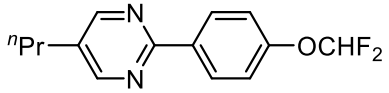

$Pd(OAc)_2$ (3.4 mg, 0.015 mmol, 5 mol%), PPh_3 (7.9 mg, 0.03 mmol, 10 mol%), K_2CO_3 (124.4 mg, 0.9 mmol, 3 equiv.) and (4-(difluoromethoxy)phenyl)boronic acid (84.6 mg, 0.45 mmol, 1.5 equiv.) were added to a flamed-dried flask. The mixture was purged with nitrogen for 5 minutes. Dioxane (0.55 mL, 0.55 M) and H_2O (0.14 mL, 2.18 M) were added, followed by 2-chloro-5-

propylpyrimidine (0.04 mL, 0.3 mmol, 1 equiv.). The reaction was then refluxed at 100 °C for 16 hours. H_2O was added to the mixture and the aqueous phase was extracted with EtOAc. The combined organics was washed with brine, dried with $MgSO_4$, and concentrated *in vacuo*. The crude mixture was purified by flash column chromatography, eluting with a 2.5 to 5% (v/v) EtOAc:pentanes gradient to give **xx** (68.5 mg, 0.26 mmol, 86%).

2-(4-(difluoromethoxy)phenyl)-5-isobutylpyridine [nementin-12-27, YHK01-118F1]

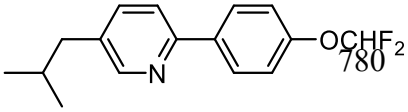

780 **xx** was synthesized according to General Procedure A, B, and C using 6-bromonicotinaldehyde, isopropyltriphenylphosphonium iodide, and (4-(difluoromethoxy)phenyl)boronic acid with an overall yield of 23%.

5-butyl-2-(4-(difluoromethoxy)phenyl)pyridine [nementin-12-27, YHK01-118F1]

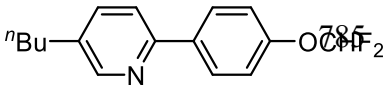

785 **xx** was synthesized according to General Procedure A, B, and C using 6-bromonicotinaldehyde, propyltriphenylphosphonium bromide, and (4-(difluoromethoxy)phenyl)boronic acid with an overall yield of 32%.

5-butyl-2-(4-methoxyphenyl)pyridine [nementin-12-28, YHK01-121F1]

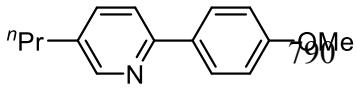

790 **xx** was synthesized according to General Procedure A, B, and C using 6-bromonicotinaldehyde, ethyltriphenylphosphonium bromide, and (4-methoxyphenyl)boronic acid with an overall yield of 41%.

4-(5-butylpyridin-2-yl)phenol [nementin-12-29, YHK01-153F1]

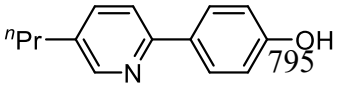

795

xx was synthesized according to General Procedure A, B, and C using 6-bromonicotinaldehyde, ethyltriphenylphosphonium bromide, and (4-(benzyloxy)phenyl)boronic acid with an overall yield of 31%.

2-(4-(2,2-difluoroethoxy)phenyl)-5-propylpyridine. [nementin-12-30, YHK01-168F1]

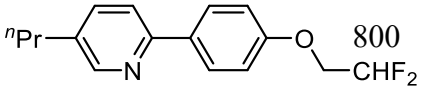

800

xx (21.3 mg, 0.1 mmol) was dissolved in DMF (0.33 ml, 0.3 M) and cooled to 0 °C. NaH (6.0 mg, 0.15 mmol, 60%, 1.5 equiv.) was added and the mixture was stirred at 0 °C for 30 minutes. 2-bromo-1,1-difluoroethane (0.02 mL, 0.15 mmol, 1.5 equiv.) was added dropwise and the reaction mixture was stirred from 0 °C to room temperature overnight. H_2O was added
805 and the aqueous phase was extracted with EtOAc. The combined organics was washed with brine, dried with $MgSO_4$, and concentrated *in vacuo*. The crude mixture was purified by flash column chromatography, eluting with 5 to 10% (v/v) EtOAc:pentanes to give **xx** (17.6 mg, 0.063 mmol, 63%).

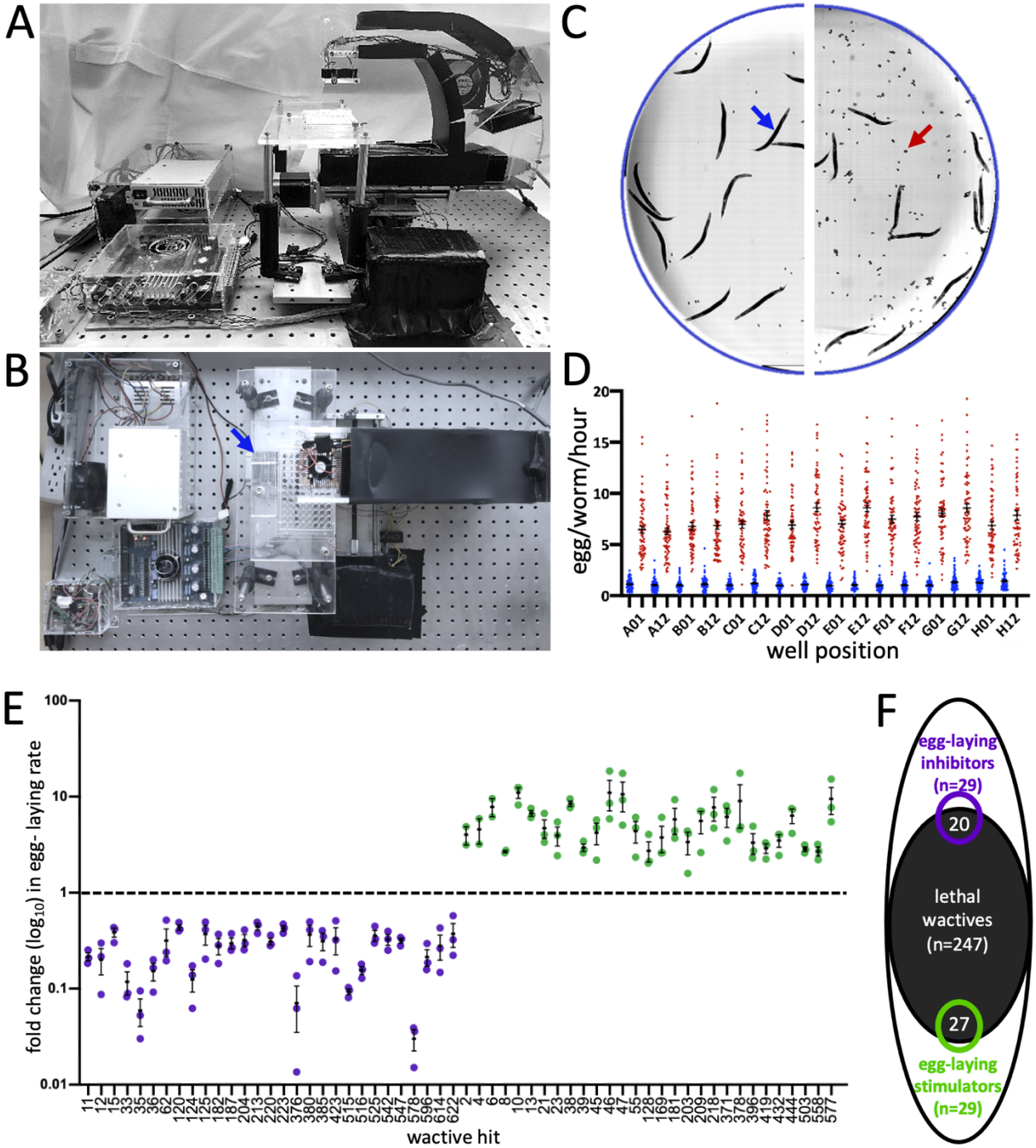

Fig. S1. The 2020 Imager enables quantification of the *C. elegans* egg-laying rate.

(**A** and **B**) Two perspectives of the '2020 Imager' showing one 96-well plate in the imager holder (arrow). (**C**) Representative half-well images of vehicle controls in the

basal (M9-only) background (left) and the 'stimulatory cocktail' of 12.3 mM serotonin
815 creatine sulfate and 7.7 mM nicotine (right) after 1 hour. A blue arrow points to an adult hermaphrodite and a red arrow points to a pair of embryos. (**D**) The distribution of counts of eggs/worm/hour for the basal background (blue) and the stimulatory background (red) from the indicated well-coordinates over 22 experimental replicates (96-well plates). The mean and SEM is shown. (**E**) A screen of the worm active
820 (wactive) library yields 29 inhibitors (purple) and 29 stimulators (green) of the *C. elegans* egg-laying rate. Mean Egl rate and SEM is shown. (**F**) Venn diagram showing the overlap of the wactive molecules that are lethal (at 60 μM) with those that modulate egg-laying among the 486 molecules assayed in both assays.

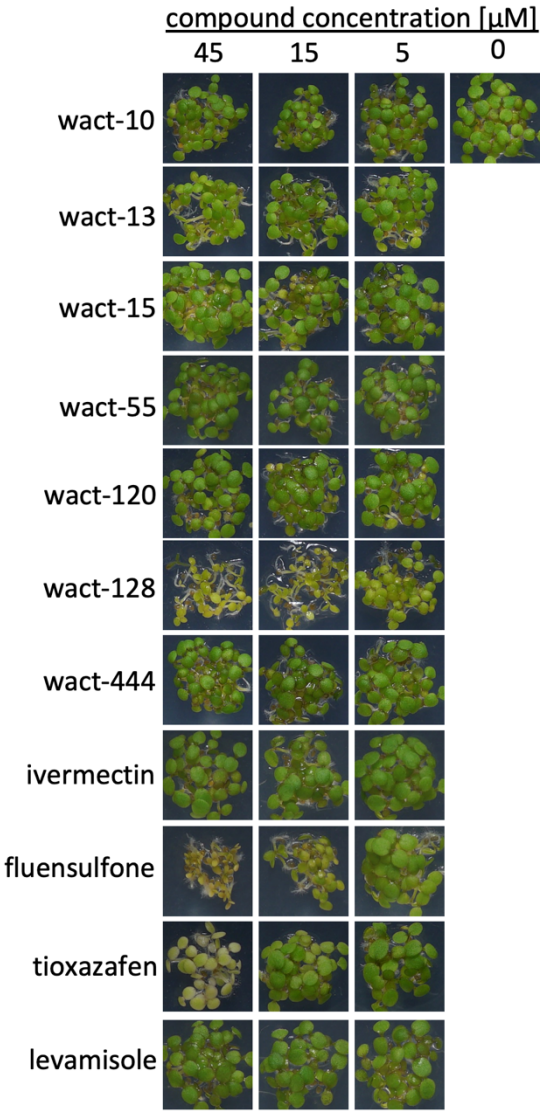

825

Fig. S2. Effect of prioritized wactives and established anthelmintics on *Arabidopsis* growth and greening. Assays were performed in 12 well polystyrene plates using 20-25 seeds per well (see Methods). Experiments were performed in triplicate. Any yellowing or obvious growth impairment was reported as activity.

830

Strain	Resistance	[Nementin-1] µM							
		0	0.94	1.88	3.75	7.5	15	30	60
N2	-	1	1	1.1	1.1	1	0	0	0
VC731 *unc-63(ok1075)*	LEV, APAs, THPs	1	1.1	1.1	1	0.8	0	0	0
CB1072 *unc-29(e1072)*	LEV, THPs	1	1	1.1	1	0.8	0	0	0
DA1316 *avr-14;avr-15;glc-1*	MCL	1	1.1	1	1	0.3	0	0	0
CB3474 *ben-1(e1880)*	Benzimidazoles	1	1	1.1	1.1	0.9	0	0	0
RB2119 *acr-23(ok2804)*	AADs	1	0.9	1.1	1	0.7	0	0	0
NM1968 *slo-1(js379)*	Emodepside	1	1.1	1.1	1	0.5	0	0	0
CF1038 *daf-16(mu86)*	Apigenin	1	1	1	1	0.4	0	0	0
RP2674 *mev-1(tr393)*	Fluopyram	1	1	1.1	0.9	0.6	0	0	0
PR1152 *cha-1(p1152)*	AChE inhibitor	1	1	1	0.9	0.2	0	0	0

Strain	Resistance	[levamisole] µM							
		0	9.38	18.8	37.5	75	150	300	600
N2	-	1	1	1	1.1	1.1	0.5	0.2	0
VC731 *unc-63(ok1075)*	LEV, APAs, THPs	1	1	1	1	1.1	1.1	1	1
CB1072 *unc-29(e1072)*	LEV, THPs	1	1.1	1.1	1.1	1	1.1	1	1
DA1316 *avr-14;avr-15;glc-1*	MCL	1	0.8	1	1	0.9	0.5	0.1	0
CB3474 *ben-1(e1880)*	Benzimidazoles	1	0.9	1	1.1	0.9	0.6	0.4	0.1
RB2119 *acr-23(ok2804)*	AADs	1	0.9	0.8	0.6	0.5	0.1	0	0
NM1968 *slo-1(js379)*	Emodepside	1	0.9	1	0.9	0.9	0.6	0.1	0
CF1038 *daf-16(mu86)*	Apigenin	1	0.6	0.9	1	0.8	0.7	0.3	0.1
RP2674 *mev-1(tr393)*	Fluopyram	1	0.8	0.9	1	0.9	0.4	0.1	0
PR1152 *cha-1(p1152)*	AChE inhibitor	1	0.3	0.2	0	0	0	0	0

Strain	Resistance	[fluopyram] µM							
		0	0.09	0.19	0.38	0.75	1.5	3	6
N2	-	1	1.1	1	0.7	0	0	0	0
VC731 *unc-63(ok1075)*	LEV, APAs, THPs	1	1	0.7	0.3	0	0	0	0
CB1072 *unc-29(e1072)*	LEV, THPs	1	0.9	0.7	0.7	0	0	0	0
DA1316 *avr-14;avr-15;glc-1*	MCL	1	1	0.9	0.2	0	0	0	0
CB3474 *ben-1(e1880)*	Benzimidazoles	1	1	0.8	0.7	0	0	0	0
RB2119 *acr-23(ok2804)*	AADs	1	1	1	0.4	0	0	0	0
NM1968 *slo-1(js379)*	Emodepside	1	1	0.6	0	0	0	0	0
CF1038 *daf-16(mu86)*	Apigenin	1	1	1	0.5	0	0	0	0
RP2674 *mev-1(tr393)*	Fluopyram	1	1.1	1.1	1	1	1.1	1	0.9
PR1152 *cha-1(p1152)*	AChE inhibitor	1	1	0.3	0	0	0	0	0

Strain	Resistance	[ivermectin] nM							
		0	1.88	3.75	7.5	15	30	60	120
N2	-	1	1	1.1	0.8	0.2	0	0	0
VC731 *unc-63(ok1075)*	LEV, APAs, THPs	1	1	1.1	1	0	0	0	0
CB1072 *unc-29(e1072)*	LEV, THPs	1	0.9	1.1	1	0	0	0	0
DA1316 *avr-14;avr-15;glc-1*	MCL	1	1	1.1	1	1	1	0.8	0.4
CB3474 *ben-1(e1880)*	Benzimidazoles	1	1	1	0.7	0.2	0	0	0
RB2119 *acr-23(ok2804)*	AADs	1	1	0.9	1	0.9	0.2	0	0
NM1968 *slo-1(js379)*	Emodepside	1	1	0.8	0.1	0	0	0	0
CF1038 *daf-16(mu86)*	Apigenin	1	1	1	0.9	0	0	0	0
RP2674 *mev-1(tr393)*	Fluopyram	1	0.9	1	1	1	0.2	0	0
PR1152 *cha-1(p1152)*	AChE inhibitor	1	0.9	0.2	0	0	0	0	0

≥ 1 — 0

number of living worms relative to DMSO control

Fig. S3. *C. elegans* strains with mutant alleles conferring anthelmintic resistance are sensitive to the effects of Nementin-1. 3-day larval development assay monitoring the development of larval stage 1 (L1) to L4/adulthood. Reporting the fraction of animals that develop to L4/adulthood relative to the solvent-only controls.

835 Data are the mean of 3 biological replicates measured in technical triplicate normalized to parallel N2 controls. Showing the strain name and genetic background of parasiticide

resistant mutants. Resistance to marketed nematode parasiticides is demonstrated for levamisole (strain VC731 & CB1072), fluopyram (strain RB2674), and ivermectin (DA1316).

840

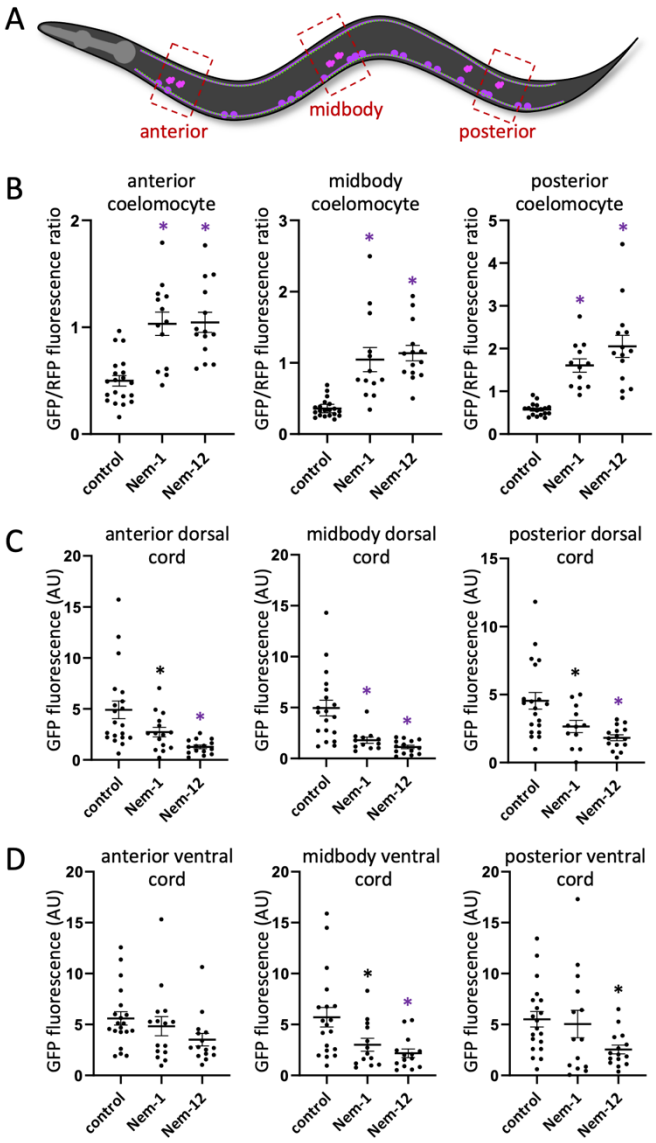

Fig. S4. Nementin treatment depletes *C. elegans* cholinergic motor neurons of neuropeptides that are released in DCVs. (**A**) Schematic of KG4247 *C. elegans* witih the *celsi201* integrated transgene expressing INS-22::GFP in cholinergic motor neurons. INS-22::GFP gets packaged into DCVs serving as a marker for DCVs. The cholinergic motor neurons of KG4247 animals also constitutively secrete mCherry, which is taken up by the coelomocytes, and serves as a coelomocyte marker (*11*). Imaged regions are

indicated with dashed red boxes. (**B-D**) Quantification of signal from the indicated cell or tissue in the indicated area of the animal. Signal is measured from coelomocytes with a
850 ratio of GFP to RFP fluorescence (because measuring GFP signal alone is too variable because of the variable size of coelomocyte endosomes). Signal is reported from the dorsal and ventral cords as the mean GFP signal with the mean surrounding background signal subtracted. Animals are treated either with DMSO-only (control) or 60 μM of Nementin for 4 hours. For all images, * $p<0.05$;** $p<0.01$; *** $p<0.001$, 1-way
855 ANOVA with Dunnett correction for multiple comparisons; means with SEM are shown.

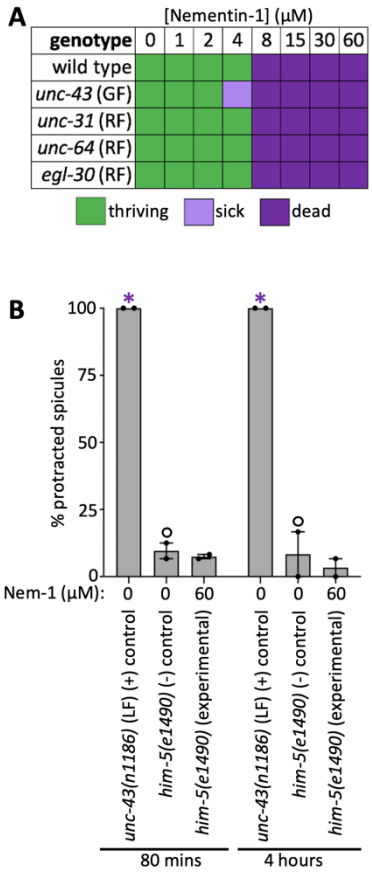

Fig. S5. UNC-43/CaMKII is unlikely to be the target of Nementin. (**A**) Six-day larval reproduction assay measuring the effects of Nementin-1 on generational development. ~20 L1s were plated per well containing 60 μM Nementin-1 in NGM media supplemented with HB101 *E. coli* as a food source with 0.6% DMSO. Thriving indicates wells are overgrown with progeny after 6-days. Sick indicates <50 L1 larvae are present per well. Dead indicates <10 live worms are present in test wells. Data are the median response of 3 biological replicates. (**B)** A test to determine whether Nementin-1 inhibits UNC-43 in its role in *C. elegans* male tail spicule protraction. The *unc-43* null mutant *(n1186)* is the positive control. The asterisk signifies Chi-Square $p<0.001$ comparing the experimental and positive control to untreated *him-5(e1490)*.

gene	ortholog	exemplar phenocopying mutation and phenotypes[a]	potential suppressing mutation and phenotypes[b]
acr-2	CHRNA1 (cholinergic receptor nicotinic subunit) (*12*)	*n2420* (GF) convulsions, Egl-c (*13, 14*)	*acr-2(ok1887)* (LF) non-Unc (*14*)
unc-2	CaV2α (voltage gated calcium channel) (*15*)	*zf35* (GF) hyperactive, convulsions (*16*)	*unc-2(e55)* (LF) sluggish (*17*)
unc-43	CaMKII (*18*)	*e408* (RF) convulsions, Egl-c (*18, 19*)	*unc-43(n498)* (GF) paralysis (*20*)
unc-58	KCNK3, KCNK9 and KCNK18 (two-pore K^+ channel) (*21*)	*e665* (GF) convulsive, Egl-c (*21*)	*unc-58(e665n273)* (LF) weak Unc (*21*)
unc-93	UNC93A (SUP-9 K^+ channel complex member) (*22*)	*e1500* (GF) rubberband (*23*)	*sup-9(n1012)* (LF) non-Unc (*22*)
sup-9	two-pore K^+ channel (*22*)	*n200* (GF) convulsive (*23, 24*)	*sup-9(n1012)* (LF) non-Unc (*22*)
sup-10	novel (SUP-9 K^+ channel complex member) (*22*)	*n983* (GF) rubber band (*23*)	*sup-9(n1012)* (LF) non-Unc (*22*)
twk-18	TWiK K^+ channel (*25*)	*e1913* (GF) lethal, rubberband, Egl-d (GF) (*26*)	*twk-18(gk5009)* (LF) non-Unc (wormbase version WS280)

Table S1.

870 **Genes that can be mutated to induce convulsions or 'rubber-band' phenotypes.**

[a]GF, gain-of-function; RF, reduction-of-function; Egl-c, constitutive egg-laying

[b]LF, loss-of-function; Unc, uncoordination.

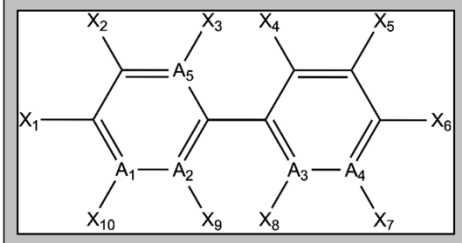

A										B						C							D				E			
										free living nematodes						nematode parasites of animals							plant parasites				non target models			
nementin analog	A_1	A_2	A_3	A_4	A_5	X_1	X_6	R	R Position	C. elegans (motor phenotype) EC50	P. pacificus (motor phenotype) EC50	Rhabditophanes sp. (motor phenotype) EC50	C. elegans (3-day larval development) EC50	P. pacificus (3-day larval development) EC50	Rhabditophanes sp. (3-day larval development) EC50	Necator americanis (L3 viability)	Trichuris muris (L1 viability)	Trichuris muris (adult viability)	Strongyloides ratti (L3 viability)	Strongyloides ratti (adult viability)	Heligmosomoides polygyrus (L3 lethality)	Heligmosomoides polygyrus (adult lethality)	M. incognita (J2 viability in vitro)	M. incognita (egg hatch rate)	M. incognita (hatchling mobility)	M. incognita (50-day soil test)	Drosophila melanogaster (45 µM highest tested)	Danio rerio (45 µM highest tested)	Arabidopsis thaliana greening (45 µM highest tested)	HEK293 EC50 (µM)
1	C	N	C	C	C	$(CH_2)_4CH_3$	OCH_3	-	-	31	25	5	9	10	2	25	nt	25	np	25	np	25	45	45	45	np	np	np	np	np
2	C	N	C	C	C	$(CH_2)_4CH_3$	$OCHF_2$	-	-	19	15	nt	15	nt	nt	10	nt	25	np	25	np	25	np	45	np	nt	nt	45	nt	nt
3	C	N	C	C	C	$(CH_2)_6CH_3$	OH	-	-	np	36	22	15	17	2	10	nt	25	np	25	25	25	45	45	45	45	np	np	np	43
4	C	N	C	C	C	$(CH_2)_7CH_3$	OH	-	-	np	>60	45	18	23	3	10	nt	25	25	25	25	25	45	45	45	np	np	np	np	35
5	C	N	C	C	C	$(CH_2)_4CH_3$	$(CH)_2CN$	-	-	>60	>60	31	3	4	2	10	nt	25	25	10	np	25	np	45	45	np	nt	15	nt	np
6	C	N	C	C	C	$(CH_2)_6CH_3$	$O(CH_2)_5CH_3$	F	X_7	np	>60	>60	np	np	np	25	nt	25	25	np	25	25	nt	nt	nt	nt	nt	nt	nt	np
7	C	N	C	C	C	$(CH_2)_4CH_3$	$(CH)_2CONH_2$	-	-	np	>60	np	>60	nt	nt	25	nt	10	25	25	25	25	nt	nt	nt	nt	nt	nt	nt	np
8	C	N	C	C	C	$(CH_2)_4CH_3$	OCH_2CH_3	-	-	np	>60	>60	4	8	2	10	nt	25	25	10	np	25	np	45	np	nt	nt	np	nt	np
9	C	N	C	C	C	$(CH_2)_2CH_3$	OCF_3	-	-	np	np	nt	38	>60	15	10	nt	25	25	25	25	25	nt	nt	nt	nt	nt	nt	nt	nt
10	C	N	C	C	C	$(CH_2)_6CH_3$	OCH_3	-	-	>60	np	np	>60	>60	>60	10	nt	25	25	10	25	25	nt	nt	nt	nt	nt	nt	nt	np
11	C	N	C	C	C	$(CH_2)_5CH_3$	OCH_3	-	-	np	nt	nt	21	nt	nt	10	nt	25	np	25	np	25	np	45	np	nt	nt	nt	nt	nt
12-1	C	N	C	C	C	$(CH_2)_2CH_3$	$OCHF_2$	-	-	5	13	7	12	21	5	25	nt	25	np	10	25	25	np	45	45	np	45	np	45	60
12-5	C	N	C	C	C	$(CH_2)_2CH_3$	$OSHF_2$	-	-	12	13	6	5	8	7	nt	25	nt	10	25	np	nt	np	45	45	np	45	np	np	60
12-6	C	C	C	C	C	$(CH_2)_2CH_3$	$OCHF_2$	-	-	np	np	47	28	22	4	25	25	nt	25	nt	25	nt	np	np	np	nt	nt	nt	nt	nt
12-7	N	C	C	C	C	$(CH_2)_2CH_3$	$OCHF_2$	-	-	9	14	5	7	8	4	nt	25	nt	25	25	np	nt	45	45	45	np	np	15	45	60
12-8	C	C	N	C	C	$(CH_2)_2CH_3$	$OCHF_2$	-	-	9	15	7	21	19	4	np	np	nt	25	25	np	nt	np	45	np	nt	nt	nt	nt	np
12-9	C	C	C	N	C	$(CH_2)_2CH_3$	$OCHF_2$	-	-	42	>60	15	31	30	8	25	25	nt	25	nt	25	25	np	np	np	nt	nt	nt	nt	np
12-10	C	N	C	C	C	CH_2CH_3	$OCHF_2$	-	-	10	18	7	12	27	4	np	25	nt	np	nt	np	nt	nt	nt	nt	nt	nt	nt	nt	np
12-11	C	N	C	C	C	CH_2	$OCHF_2$	-	-	30	29	17	29	32	18	np	25	nt	np	nt	np	nt	np	45	np	nt	nt	nt	nt	np
12-12	C	N	C	C	C	H	$OCHF_2$	-	-	33	>60	32	35	31	9	np	25	nt	25	nt	np	nt	45	45	np	np	nt	nt	nt	np
12-14	C	N	C	C	C	$CH_3(C)_2$	$OCHF_2$	-	-	14	12	5	>60	>60	6	25	np	nt	np	nt	np	nt	np	45	np	nt	nt	nt	nt	np
12-17	C	N	C	C	C	CH_2NH_2	$OCHF_2$	-	-	np	np	>60	np	np	>60	25	25	nt	np	nt	np	nt	np	np	np	nt	nt	nt	nt	np
12-20	C	N	C	C	C	H	$OCHF_2$	$(CH_2)_2CH_3$	X_{10}	np	>60	27	np	np	50	np	10	nt	np	nt	np	nt	nt	nt	nt	nt	nt	np	nt	60
12-21	C	N	C	C	C	H	$OCHF_2$	$(CH_2)_2CH_3$	X_2	53	np	17	38	np	6	25	10	nt	np	nt	np	nt	np	np	np	np	nt	nt	nt	nt
12-22	C	N	C	C	C	H	$OCHF_2$	$(CH_2)_2CH_3$	X_3	>60	np	36	np	>60	17	np	25	nt	np	nt	np	nt	nt	nt	nt	nt	nt	nt	nt	nt
12-23	C	N	C	C	C	$(CH_2)_2CH_3$	H	$OCHF_2$	X_5	13	np	18	28	np	4	np	10	nt	np	nt	np	nt	np	np	np	nt	nt	np	nt	60
12-24	C	N	C	C	C	$(CH_2)_2CH_3$	H	$OCHF_2$	X_4	np	np	>60	>60	np	>60	nt	nt	nt	nt	nt	nt	nt	nt	nt	nt	45	np	np	45	60
12-25	C	N	C	C	N	$(CH_2)_2CH_3$	$OCHF_2$	-	-	20	30	10	8	18	6	25	25	nt	np	nt	np	nt	np	45	45	45	np	45	45	60
12-26	C	N	C	C	C	$CH_2CH(CH_3)_2$	$OCHF_2$	-	-	22	35	2	15	21	19	np	25	nt	25	25	np	nt	np	45	np	45	np	45	np	np
12-27	C	N	C	C	C	$(CH_2)_3CH_3$	$OCHF_2$	-	-	11	15	4	15	11	4	25	25	nt	np	nt	np	nt	np	45	45	45	np	np	np	60
12-28	C	N	C	C	C	$(CH_2)_2CH_3$	OCH_3	-	-	19	22	6	11	12	2	np	25	nt	25	nt	25	nt	45	45	45	np	np	15	45	60
12-29	C	N	C	C	C	$(CH_2)_2CH_3$	OH	-	-	np	np	52	np	>60	59	25	np	nt	np	nt	np	nt	np	np	45	45	45	45	np	np
12-30	C	N	C	C	C	$(CH_2)_2CH_3$	$OCHCH_3CHF_2$	-	-	np	np	6	4	8	2	nt	nt	nt	nt	nt	np	nt	nt	nt	nt	45	np	np	np	np
13	C	N	C	C	C	$(CH_2)_6CH_3$	$OCHF_2$	-	-	>60	>60	18	48	44	2	25	nt	25	25	25	25	25	45	np	np	45	np	np	np	np
14	C	N	C	C	C	$(CH_2)_4CH_3$	I	-	-	>60	np	56	>60	>60	2	10	nt	25	nt	25	np	25	np	np	45	np	np	np	np	np
15	C	N	C	C	C	$(CH_2)_4CH_3$	Br	-	-	>60	>60	31	>60	>60	2	10	nt	25	25	25	np	25	np	45	np	nt	nt	nt	nt	np
16	C	N	C	C	N	$(CH_2)_7CH_3$	OH	-	-	np	>60	44	17	25	5	25	25	nt	np	nt	np	nt	45	45	45	np	nt	nt	nt	60
17	C	N	C	C	N	$(CH_2)_5CH_3$	H_2N	-	-	58	22	20	32	28	2	nt	25	nt	10	25	25	nt	45	45	45	np	nt	45	nt	55
18	C	N	C	C	N	$(CH_2)_3CH_3$	Br	-	-	>60	np	>60	7	9	5	25	25	nt	np	np	25	nt	45	45	45	np	np	45	np	np
levamisol										48	32	44	32	48	44	10	10	10	10	10	10	10	nt	nt	nt	nt	np	np	np	np
ivermectin										<2	<2	2	<2	<2	2	10	10	10	10	10	10	10	nt	nt	nt	nt	5	<4	np	nt
fluopyram										<2	<2	3	<2	1	3	nt	nt	nt	nt	nt	nt	nt	45	45	45	45	np	np	15	np
tioxazafen										5	4	<2	4	5	<2	nt	nt	nt	nt	nt	nt	nt	45	45	45	45	np	np	45	np
oxamyl										nt	nt	nt	nt	nt	nt	nt	nt	nt	nt	nt	nt	nt	np	45	45	45	5	25	np	np
iprodione										np	>60	60	>60	np	60	nt	nt	nt	nt	nt	nt	nt	nt	nt	nt	np	15	45	nt	np
solvent										np	np	np	np	np	np	np	np	np	np	np	np	np	np	np	np	np	np	np	np	np

free-living nematode potency (µM): 0 – ≥60

nematode parasite activity scale (colour represents % of animals with phenotype): <20 | >20<50 | >50

non-target model activity scale (%): <20 | >20<50 | >50

Table S2. Nementin structure-activity relationship analysis. (**A**) The analog structures are represented by the Markush structure at the top and includes atom and substituent identifiers. (**B**) Data for the free-living nematodes are EC50s (μM) and color-coded based on the potency scale at the bottom of this section. (**C** and **D**)**.** Nematode

parasites of mammals or plants were tested with a limited number of compound
880 concentrations. In each cell in these sections, the lowest concentration (μM) tested that exhibited a phenotype is shown, and the percentage of animals that exhibit the phenotype is indicated by the colour scale at the bottom of this section. (**E**) Data for models of non-targeted systems is reported either as an EC50 (μM) (for the HEK293 cells) or as the lowest concentration tested (μM) that exhibited a discernible phenotype
885 compared to wild-type at the indicated concentration; the percentage of animals that exhibit the phenotype is indicated by the colour scale at the bottom of this section. np, no phenotype (< 20% effect); nt, not tested. See the Methods for a description of each assay.

890 **Movie S1.**

Example of typical wild type *Caenorhabditis elegans* locomotion. Wild type *C. elegans* (strain N2) are swimming on solid media containing only 1% DMSO solvent control that is incorporated into the agar. Animals have been swimming on the plate for 80 minutes at the time the movie was made.

895

Movie S2.

Example of compound-induced convulsions. Wild type *C. elegans* (strain N2) are shown after swimming on solid media containing 60 μM Nementin-1 for 80 minutes.

900 **Movie S3.**

Example of compound-induced coiling. Wild type *C. elegans* (strain N2) are shown after swimming on solid media containing 60 μM wact-45 for 80 minutes.

Movie S4.

905 **Example of compound-induced shaking.** Wild type *C. elegans* (strain N2) are shown after swimming on solid media containing 60 μM Nementin-1 for 80 minutes. At the 18 second mark of the movie, *C. elegans* (strain N2) are shown after swimming on solid media containing 60 μM wact-203 for 80 minutes. At the 21 second mark of the movie,

wild type *Rhabditophanes diutinus* animals are shown after swimming on solid media
910 containing 60 μM Nementin-1 for 170 minutes.

Movie S5.

Example of compound-induced jerky-unc phenotype. Wild-type *C. elegans* (strain N2) are shown after swimming on solid media containing 60 μM wact-45 for 80 minutes.

915

Movie S6.

Example of compound-induced reversal-defective phenotype. Wild type *C. elegans* (strain N2) are shown after swimming on solid media containing 60 μM wact-38 for 80 minutes.

920

Data S1. (Separate file)

Egg-laying rates with and without a stimulatory cocktail.

925 **Data S2. (Separate file)**

The Wactive Library egg-laying screen data.

Data S3. (Separate file)

The locomotory survey of the egl-modulators.

930

Data S4. (Separate file)

Nematode and Counter-Screen Bioassay Data.

935